

NEAR INFRARED NONINVASIVE OPTICAL IMAGING (NIR NOISE) ON
OBJECTS HIDDING IN A SCATTERING MEDIUM

THESIS

Presented to the Graduate Council of
Texas State University-San Marcos
in Partial Fulfillment
of the Requirements

for the Degree

Master of SCIENCE

by

Elaine E. Tennant, B.S.

San Marcos, Texas
August 2007

ACKNOWLEDGEMENTS

First I would like to thank Wilhelmus J. Geerts. He has taught me a large and invaluable amount of information. He has gone above and beyond the duties of a thesis advisor and I truly appreciate everything he has done for me.

Secondly I would like to thank Zvi Yaniv for giving me the opportunity to participate in this project. Without his support it would not have been possible.

I would like to thank the other members of my committee, Thomas Lawrence and Dan Tamir. They both have been a great help to me.

A huge thank you goes to Chris O'Brien for helping me with programming and being an excellent problem solver.

I would like to thank Matthew McDougale for helping with the FTIR measurements.

I would especially like to thank the Texas State University-San Marcos Department of Physics. From the first day I arrived here I have been welcomed into their community. They have given me an education, a job and support.

Much of the credit for my success belongs with my parents, Richard and Aimee Tennant. I would like to thank them not only for the financial support but for everything else they have given me.

Most of all I want to thank my husband Daniel Fletcher. Thanks Danny, Thanny.

This manuscript was submitted July 26, 2007.

TABLE OF CONTENTS

	Page
ACKNOWLEDGEMENTS	iii
LIST OF TABLES	vii
LIST OF FIGURES.....	viii
ABSTRACT	xii
CHAPTERS	
1 INTRODUCTION.....	1
1.1 Speckles.....	1
1.2 Images	3
1.3 Scattering.....	4
1.4 NOISE Basics.....	9
2 MEDICAL BACKGROUND AND MOTIVATION	12
2.1 X-ray Imaging	12
2.2 Magnetic Resonance Imaging	14
2.3 Ultrasound Imaging.....	14
2.4 Positron Emission Tomography	15
2.5 NOISE	15
3 OPTICS BACKGROUND.....	17
3.1 Principles of Scattering	17
3.2 Absorption versus Scattering	18
3.3 Point Spread Function and Symmetry.....	28
3.4 Scattering Effects Due to Each Component.....	31
4 NOISE SYSTEM	34
4.1 System Specifications and Theory	35
4.2 Multi-Lens-Array Concerns	37
4.3 System Configuration.....	42
5 BIOLOGY	47
5.1 Cells	47

5.2	Biological Effects on Scattering.....	50
5.3	Analysis of Chicken	54
6	PROGRAMMING	61
6.1	Shift and Add	61
6.2	Isomorphisms and Frequency Space	64
6.3	Program Specifics	69
7	NOISE IN THE NEAR INFRARED REGION	76
7.1	Final Configuration	76
7.2	Voltage Variance	77
7.3	Thickness of the Scattering Medium	78
7.4	Red vs. Near Infrared	79
8	DISCUSSION AND CONCLUSIONS.....	82
	APPENDIX A – SYMBOLS	84
	APPENDIX B – LABVIEW.....	85
	WORKS CITED.....	88

LIST OF TABLES

	Page
Table 2.1: Typical scan doses of imaging scans	13
Table 3.1: vibrational transitions depending of the molecular bond and elements.....	19
Table 3.2: scattering and absorption coefficients of various biological tissue.....	27
Table 5.1: refractive indices of various cellular structures	52

LIST OF FIGURES

	Page
Figure 1.1: Speckle image from image processing book	2
Figure 1.2: No image formation as light from many points of the object will contribute to the intensity at P.	2
Figure 1.3: Pinhole camera resulting in a one to one relation between points of the object and the image.	4
Figure 1.4: Lens as an image forming device.	4
Figure 1.5: Interference in the absence of a scattering media.	5
Figure 1.6: Interference when a scattering media is present.	5
Figure 1.7: (a): speckle interferogram of the binary star ψ -Sagittarii. (b): the same star after a speckle processing method	6
Figure 1.8: Jul 20, 2006; object embedded	7
Figure 1.9: Speckle pattern created by surface roughness.	7
Figure 1.10: capturing light scattered at different angles.....	9
Figure 1.11: Left, speckle image taken with chicken breast. Right, extracted image.....	10
Figure 2.1: An X-ray picture taken by Wilhelm Röntgen in 1896, of Albert von Kolliker's hand	12
Figure 3.1: geometrical cross section of an absorbing element	20
Figure 3.2: geometrical cross section of a scattering element.....	22

Figure 3.3: several elements of a scattering event	23
Figure 3.4: spherical scatterer of uniform refractive index.....	24
Figure 3.5: Normalized Scattered Intensity as a function of the Deflection angle for a 304 nm diameter polystyrene sphere in water taken with a 633 nm laser	25
Figure 3.6: light path through front and back scatterers	29
Figure 3.7: symmetric light path through a cell	29
Figure 3.8: elements of the NOISE system	31
Figure 3.9: cross with back scattering, illumination provided by red laser	33
Figure 4.1: floor plan of setup.....	34
Figure 4.2: object, image distance.....	35
Figure 4.3: ray diagram of the field of view of the MLA.	36
Figure 4.4: each lens of the MLA captures a different bit of scattered.....	38
Figure 4.5: picture taken with the MLA without scattering.....	39
Figure 4.6: picture of object embedded in chicken while being agitated.....	40
Figure 4.7: image on the left is taken from the outer edge of the array; image on right is taken from the center of the array	40
Figure 4.8: configuration of the camera connection to the computer.	43
Figure 4.9: image that maximizes the number of channels but has visible edge effects ..	44
Figure 4.10: image that reduces edge effects; however this severely limits the number of channels.....	45
Figure 4.11: final setup; maximizes usable channels while minimizing edge effects.	45
Figure 4.12: summed picture of above array.....	46
Figure 4.13: system design.....	46
Figure 5.1: diagram of a cell	48
Figure 5.2: the therapeutic window exists where the absorption coefficient is minimized	

with respect to wavelength	50
Figure 5.3: absorption coefficients of various biological structures with respect to wavelength	51
Figure 5.4: scatter intensity with respect to the scatter angle. Notice that melanin has a higher scattered intensity.....	52
Figure 5.5: as the size of the nucleus increases so does the scattered intensity	53
Figure 5.6: scattering of a cell with and without organelles	54
Figure 5.7: transmission with respect to wavelength of 2mm of chicken.....	56
Figure 5.8: as thickness of the chicken increased the overall transmitted light decreased. There is still a clear trend with respect to wavelength	57
Figure 5.9: effect of small variations in thickness on transmission	57
Figure 5.10: these measurements were taken with different types of chicken tissue (fat, muscle.)	58
Figure 5.11: ftir and filmetrics data.....	59
Figure 5.12: transmission of beef versus chicken	59
Figure 5.13: left is chicken breast; right is lean turkey; both are raw. Note that the textures are different.....	60
Figure 6.1: the difference between the two x's will produce a fuzzy final image.....	62
Figure 6.2: height and length of one channel; image taken with scattering.....	62
Figure 6.3: image taken without scattering for calibration	63
Figure 6.4: bobcat imaged through the MLA without scattering. The slight edges that are visible in each channel are due to the diaphragm in front of the MLA.....	69
Figure 6.5: the image inside the hexagon can be contained in a rectangle	70
Figure 6.6: grid length.....	70
Figure 6.7: user interface for the grid calibration program	71
Figure 6.8: the corners of the rectangle all lie on the same feature of the object.....	71

Figure 6.9: summed image.....	72
Figure 6.10: user interface for the ‘shift and add’ program, NOISE1.	73
Figure 6.11: angle of rotation.....	73
Figure 6.12: the initial channel that the user selects needs to be in the bottom left corner.	75
Figure 7.1: the front scatterer is the scattering element that is closest to the laser. The back scatterer is the scattering element closest to the camera.....	77
Figure 7.2: copper object with "hook".	77
Figure 7.3: picture of hook taken with 100mV.	78
Figure 7.4: picture of hook taken with 200mV.	78
Figure 7.5: 400 mV.	78
Figure 7.6: 800mV.	78
Figure 7.7: square object with a small identifying feature.....	78
Figure 7.8: 4 layers of front scattering; 1 layer of back scattering	79
Figure 7.9: 2 layers of front scattering; 1 layer of back scattering	79
Figure 7.10: 2 layers of chicken before and after then object, about 2.5 cm of chicken ..	79
Figure 7.11: picture of object embedded in chicken illuminated by red laser	80
Figure 7.12: yoyo object with paper front scattering	80
Figure 7.13: 2 layers of front scattering and 1 layer of back scattering	81
Figure 7.14: 4 layers of back scattering, 1 layer of front scattering	81
Figure 7.15: 3 layers of front scattering and 2 layers of back scattering taken with 685 nm laser.	81
Figure 7.16: square object with 3 layers of front scattering and 2 layers of back scattering taken with 808 nm laser.	81
Figure 8.1: red laser directed at cubic beam splitter.	83

ABSTRACT

NEAR INFRARED NONINVASIVE OPTICAL IMAGING (NIR NOISE) ON OBJECTS HIDDING IN A SCATTERING MEDIUM

by

Elaine E. Tennant, B.S.

Texas State University-San Marcos

August 2007

SUPERVISING PROFESSOR: WILHELMUS GEERTS

Non-invasive optical imaging by speckle ensemble (NOISE) is a technique for taking an image of an object while it is embedded between two scattering mediums. These mediums can be anything from smoke to frosted glass to biological tissue. The images taken of the object are speckled because of the scattering of the light by the medium surrounding the object. In order to reduce the effect of the scattering we have taken multiple images from different direction using a multi lens array. After running an

algorithm that averages all the images together, the scattering has been compensated for and the object becomes obvious.

These methods have applications in medical, military and even law enforcement fields. Human tissue is an appropriate scattering medium and has an added benefit of being partially transparent to light in the near infrared spectrum. This property can be exploited for medical purposes.

We have built a NOISE setup at our University that works in the near infrared and have used it to study binary objects embedded in chicken meat (used to simulate human tissue). Our setup has a smaller surface area than Dr. Rosen's (eight sq. ft. versus thirty two sq. ft.) It also includes two diaphragms that were not included in Dr. Rosen's setup. Images were also taken with different scattering mediums with two different wavelengths of light. An image was extracted from a picture of an object embedded in three cm of chicken meat, which is a thicker scattering medium than Dr. Rosen used. The optical properties of the chicken breast were measured using two different methods. Two separate programs were written to deal with the speckle processing, as well as a real-time version. These results as well as the constructed setup will be discussed.

CHAPTER 1

INTRODUCTION

NOISE uses a speckle imaging process. This process has several parts, the speckling of the image, how and why information can be extracted from speckles and the computations and algorithms involved in extracting those images. This paper will talk about how each of those aspects were studied and applied to the NOISE system. It will also address the physical configuration of the system and the scattering mediums that were used.

1.1 Speckles

A speckle image is an image of an object formed by light that has been transmitted through an inhomogeneous scattering medium. The medium has to contain an inhomogeneous mixture of different materials all with low to no absorption and all with different refractive indices to randomize the light's path through the medium. As light travels from one of the materials to the next it is repeatedly scattered in different directions. Each time light is scattered the phase is effected, so depending on the path it travels through the medium the light will experience a different phase shift. This randomizes the phase of each separate bit of light, of each different ray.

When these different rays are combined together in an image, their electric fields do not always add constructively, but in some cases destructively. The resulting image is a superposition of these electric fields. Where the waves add destructively there are dark areas and where they add constructively there are light areas. This process results in an interference pattern. The interference pattern is then superimposed on an image of the same object without a scattering medium present. This is known in image processing as speckle noise. Speckle noise is not easy to remove since it is not additive, but depends on the brightness of the pixels of the picture. The brighter parts of the image will have a larger noise component, while the noise in the darker areas of the image will be significantly lower. If the object is described by a two dimensional function, $u(x,y)$, the image, $v(x,y)$, is given by¹²:

$$v(x, y) = u(x, y)s(x, y) + \eta(x, y) \quad [1.1]$$

Where $\eta(x,y)$ is zero average Gaussian white noise field, and $s(x,y)$ is the speckle noise intensity which is a white noise random field with exponential distribution, i.e¹².

$$p_s(\xi) = \frac{1}{\sigma^2} e^{-\xi/\sigma^2} \quad \text{for } \xi \geq 0$$

$$p_s(\xi) = 0 \quad \text{for } \xi < 0$$
[1.2]

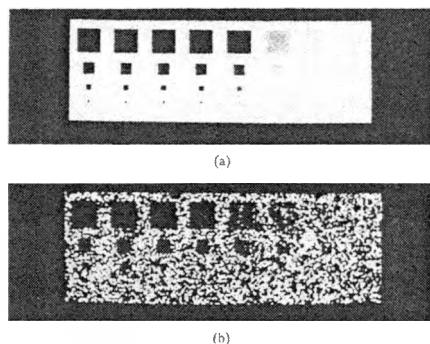


Figure 1.1: Speckle image from image processing book.

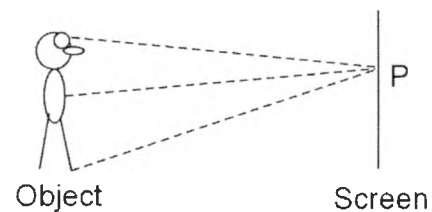


Figure 1.2: No image formation as light from many points of the object will contribute to the intensity at P.

Speckle noise can be described as multiplicative. This can also be seen in Fig. 1 below. The squares with the higher intensity have the larger noise while the darker areas have very little speckle noise.

1.2 Images

An image is a one to one correspondence between an object and an image formed of that object. That means that for every point on an object, there is only one point on the image. If more points on the object map to the same point on the image, the result can be a fuzzy blur or in the worst case not a formation of an image. Just putting an object in front of a screen would not result in the formation of an image of the object on the screen (see Fig. 1.2). If the points on an object mapped to nowhere in the image, the image would be dark (the null image) or obscured. This is not a good representation of the object, however. Taking an image is a more complicated process than simply exposing a detector to light. There has to be some physical device that organizes that one to one mapping.

The simplest device to provide this mapping, or focus, is the pinhole camera. By geometry, this device restricts the rays of light coming off an object, only allowing a single ray per point to be imaged (see Fig. 1.3).

The most commonly used image creating device is a lens. Lenses direct light so that incoming light rays are kept in the same organization but often flipped or reversed. So there is still a one to one relation between points of the object and points of the image.

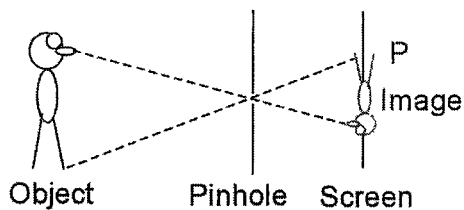


Figure 1.3: Pinhole camera resulting in a one to one relation between points of the object and the image.

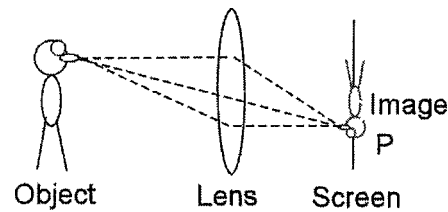


Figure 1.4: Lens as an image forming device.

A camera using a lens is more sensitive than a pinhole camera since for each object point a lot of rays travel from object to image (see Fig. 1.4). For the pinhole camera there is only one ray that will reach the screen for each point of the object. All other rays are blocked out which makes the pinhole camera very insensitive (see Fig. 1.3).

1.3 Scattering

These imaging methods do not involve random scattering so the light is all in phase even if some light traveled further than others. This type of image is one the populace are used to seeing, clear, definitive and closely resembling the object.

If coherent light is used to illuminate the object, the electric field at each point of the image can be expressed as a summation of the electric field contributions of each ray (see Fig. 1.4). Although the path length of each ray is different, the optical path length (the travel time) of each ray is the same, so all rays will have the same phase, δ . Using complex notation, the total electric field at point P of the image can then be expressed as:

$$E_{total} = \sum_{j=1}^N A_j e^{i\delta_j} \quad [1.3]$$

When a scattering medium is introduced to the system, the phase of the electric field is effected. There is no simple linear relationship between the electric field at the object and the electric field at the image. The different rays in Fig. 4 will all have their own random phase shift δ_j . The total electric field at point P of the image can now be expressed as:

$$E_{total} = \sum_{j=1}^N A_j e^{i\delta_j} \quad [1.4]$$

If we assume that the phase shift δ_j is random for each ray, the electric fields of the different rays no longer add constructively. Figure 1.5 and 1.6 below show what happens to the total complex electric field vector in a coherent imaging system in the absence of a scattering media (Fig. 1.5) and when a scattering media is present (Fig. 1.6).

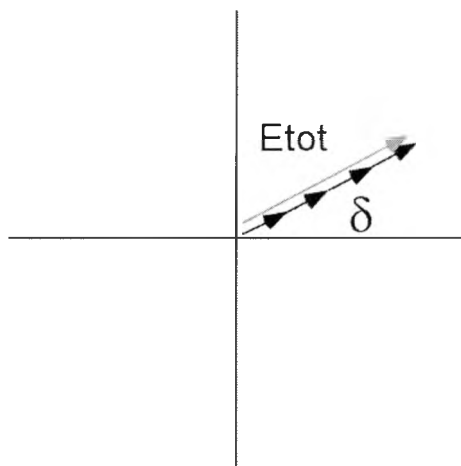


Figure 1.5: Interference in the absence of a scattering media.

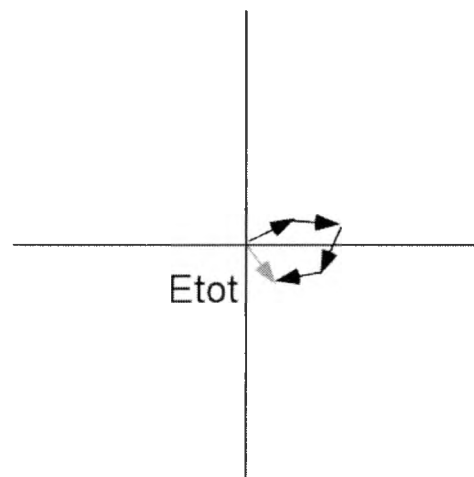


Figure 1.6: Interference when a scattering media is present.

This variable describes the real and complex parts of the wave. As the wave recombines, the electric field combines destructively creating dark spots and constructively in others, creating light spots. These are the light and dark spots of a speckle pattern. If we assume that each ray has a random phase, it can be shown that the intensity distribution of a speckle image is given by the above equations [1.1] and [1.2].¹³

Astronomy is one of the fields that have to deal with speckles. Earth's atmosphere is an appropriate scattering medium; the twinkling of stars is simply light being scattered through the ionosphere. Figure 1.7a shows a speckle image of the binary star ψ -Sagittarii taken by a telescope on earth. This image can be processed using a speckle masking technique (see Fig. 1.7b.)

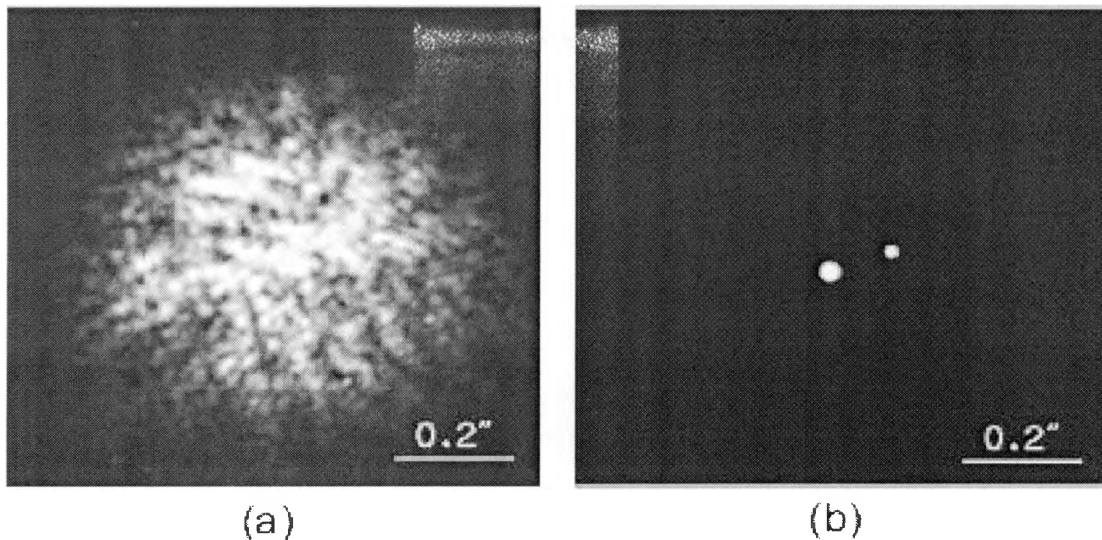


Figure 1.7: (a): speckle interferogram of the binary star ψ -Sagittarii. (b): the same star after a speckle processing method. The scale segment is equal to 0.2 as.¹³

Another scattering medium that creates speckles is biological tissue. Not only is it macroscopically inhomogeneous (bone, blood, muscle, etc) it is also microscopically inhomogeneous. Every cell contains various organelles (nucleus, mitochondria,

ribosome, etc) suspended in cytoplasm, each with their own refractive index. The scattering medium used in this research was chicken breast. An example of a speckled image from a binary object sandwiched between chicken breasts is shown in Fig. 1.8.

Speckles can also be formed without an inhomogeneous transfer medium. If the object to be imaged has a roughness comparable to that of the wavelength of the used light, and coherent monochromatic light is used to image the object, the image will contain speckles. Fig. 1.9 shows a speckle image from a laser beam pointer taken with a camera.

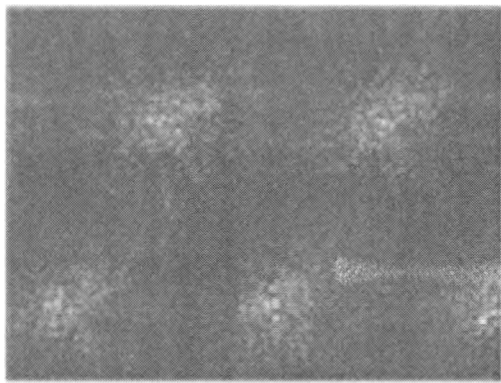


Figure 1.8: Jul 20, 2006; object embedded in chicken breast.

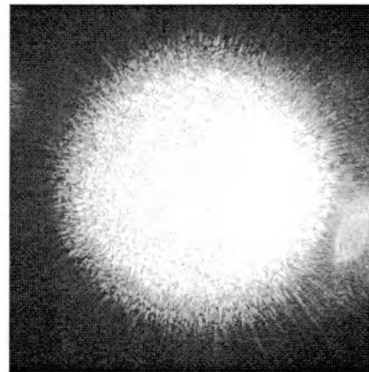


Figure 1.9: Speckle pattern created by surface roughness.

Speckle imaging is the field that studies speckles in order to avoid them in the image or to extract information from the speckle pattern about the object or scattering media. There are several techniques to reduce the effect of speckles in the image. The basis of all speckle imaging is being able to average pictures of the same object with slightly different scattering in the intensity domain. As the phase has not an influence on the intensity of an individual

speckle, the speckle noise can be significantly reduced by adding up intensity pictures taken at slightly different times or slightly different angles. This is similar to flipping a coin, if only a small number of flips are taken into consideration the coin might turn up all heads or all tails, but when a large number of flips is considered the number of heads and tails will get close to 50-50. A common technique is to take many consecutive pictures with a scattering medium that changes slightly with respect to time. Because of weather patterns the ionosphere fluctuates with respect to density and width. If a picture was taken every second, the speckle pattern would be different every time because the scattering medium would not be the same every time. When these pictures are averaged over time a quality image can be extracted. This makes astronomy an excellent field to use speckle imaging. An example is given in Fig. 1.7b which shows the speckle reduction of averaging pictures taken at different times with an telescope on earth.

With several different speckle patterns of the same object, it is possible to extract a good image of the object. This is because the “random” scattering is not completely random. All the light has to be scattered in the same way; that is to say, the frequencies at which the light is scattered must be the same. This means that the light used in speckle imaging must be coherent. The randomness comes from the amount that light is scattered. By using biological tissue, there is a randomness about how thick the scattering medium is and how inconsistent it is.

1.4 NOISE Basics

NOISE works with time-independent, angle-dependent image manipulation. This process takes pictures of an object through scattering medium at different angles, each angle grabbing a different section of the scattered light. This provides the difference between the speckle patterns that is necessary for the extraction algorithm to work. To do this a multi-lens array is used, which is an array of lenses spread out over a large glass substrate.

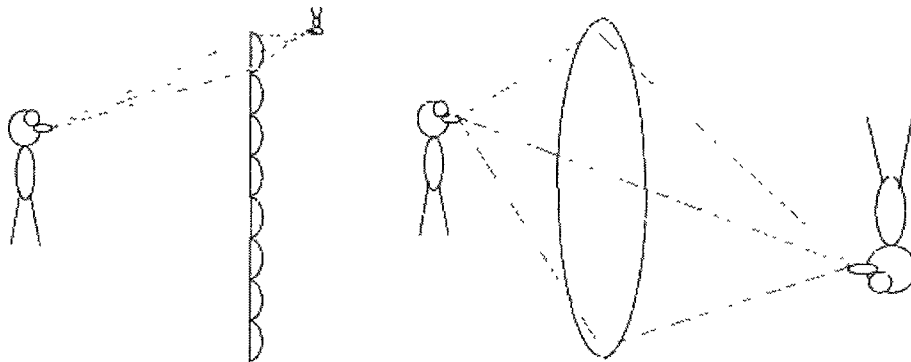


Figure 1.10: capturing light scattered at different angles.

Each lens of the MLA uses a small cone of the light coming from the object, one that has been scattered in a particular direction. This light is close to being in phase with itself, although each lens' image is not in phase with each other. So most likely each image is less speckled than the overall image. Also, at this point the intensities are being averaged, not the electric fields, so the phase shift has already been dealt with.

Dr. Rosen, et al. did preliminary research on this project. They constructed a NOISE system using a MLA and a large lens for focus. Their system was built on a 4x8 feet optical isolation vibration table and is thus 32 square feet. They used chicken breast as a scattering medium. The pictures shown in Fig. 1.11 were taken with front and back scattering and the cross on the right is the image was extracted using their program. They wrote two programs for extracting an image, NOISE1 and NOISE2. NOISE1 is a shift and add algorithm that takes each image formed by a single lens of the MLA and shifts it onto the image next to it ad infinitum, then adds all of the images. NOISE2 uses an image registration technique to locate each image of the object and uses those coordinates to add them. This solves most of the problems that are inherent in using the MLA. The Rosen group also confirmed that coherent light was necessary for this process.

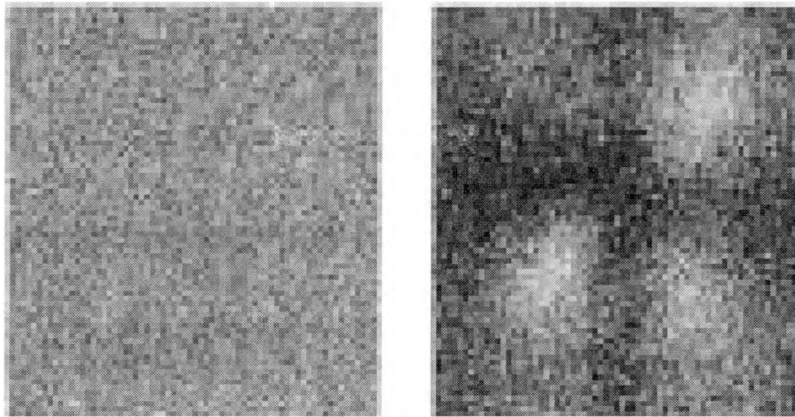


Figure 1.11: Left, speckle image taken with chicken breast. Right, extracted image.¹⁴

The NOISE system that we constructed has a significant smaller floor plan, i.e. 4 square feet. The large lens that was used by the Rosen group was not used in this setup. We included two diaphragms also not used by the Rosen group. Furthermore we took images with 3 different lasers, 632.8nm, 685nm and 808nm. The 808nm laser is in the

near infrared range. Using this laser exploits the optical properties of biological tissue, maximizing scattering while minimizing absorption. Images were taken with three cm of chicken meat, a thicker medium than used by the Rosen group. Two separate Labview programs to average the images were written. The first included a shift algorithm to separate each image from the array and stack them on top of each other, then add. The second includes a convolution of the array that has been through a scattering medium and a point spread function that defines the spacing of the array. This method of imaging would be cheaper and less invasive than current medical imaging techniques. The theoretical and mathematical work for this method will be discussed. The various setups that were used and programs that were designed to extract meaningful data from the images taken will be thoroughly detailed.

CHAPTER 2

MEDICAL BACKGROUND AND MOTIVATION

There are many different current medical imaging systems. While these methods are for the most part extremely accurate, most of them are inconvenient, costly and some are invasive.

2.1 X-ray Imaging



Figure 2.1: An X-ray picture taken by Wilhelm Röntgen in 1896, of Albert von Kolliker's hand.

An x-ray image is taken by exposing a body part to electromagnetic radiation with a wavelength of 10-01 nm. By placing a photographic plate behind the body part a silhouette of the bone structure will be imaged. This is a two dimensional image. An x-ray image takes time to develop since it is imaged by a photographic plate (see Fig. 2.1). Often it is necessary for an x-ray image to be

examined by a radiologist who specializes in interpreting these images which takes more time. X-rays are in the category of ionizing radiation and thus the total use of X-

rays on the same patient is limited. The table below gives some typical exposure levels.

One x-ray system, the Optima URS plus LP costs \$45,125.

There are special X-ray systems that can determine a three-dimensional image of a body part. Computed Tomography (CT scans or CAT scans) is such an imaging technique. This is a three dimensional scanner. By taking multiple two dimensional x-ray scans of a body from all sides and through a data manipulation process known as windowing, this method produces extremely accurate three dimensional images. It is expensive and exposes the tissue to high doses of ionizing radiation and can thus be harmful if overused. These machines generally cost between \$400,000 and 1.5 million dollars.

Table 2.1: Typical scan doses of imaging scans.

Examination	Typical <u>effective dose</u> (mSv)
	1 Sv is equal to 100 rem
Chest X-ray	0.02
Head CT	1.5(a)
Abdomen	5.3(a)
Chest	5.8(a)
Chest, Abdomen and Pelvis	9.9(a)
Cardiac CT angiogram	6.7-13(b)
CT colongraphy (virtual colonoscopy)	3.6 - 8.8

2.2 Magnetic Resonance Imaging

A magnetic resonance scanner (MRI) uses huge magnetic fields and radio waves to image organs or objects in the body. An MRI machine is expensive; costing roughly one million dollars per Tesla with scanners usually ranging from .3 to 3 Teslas, this ends up as \$350,000 to 4 million dollars⁴. It also costs several thousand per year for upkeep⁴. Another consideration for these machines is the massive magnetic field they generate. This makes it impossible for use by people with any type of metal implant, such as pacemakers.

2.3 Ultrasound Imaging

Ultrasound generally refers to the medical technique of imaging using sounds ranging from 1 to 2 MHz. This method uses a type of sonar. When sound encounters different layers of tissue, part of the sound wave is reflected. These reflections are detected and used to create an image, by differentiating the direction the reflected wave is moving, how long it took the wave to be reflected (or how far the wave traveled) and how much of the wave was reflected. This technique is commonly used in obstetrics to look at fetuses while they are in the womb. It is a non-invasive procedure with no exposure to ionizing radiation. The resolution of this system varies with respect to the wavelength of sound; longer wavelengths have less resolution but greater penetration depth than shorter wavelengths. A typical system costs between 100 and 250 thousand dollars.

2.4 Positron Emission Tomography

A positron emission tomography scan (PET scan) produces a three dimensional function of a system over time. This is done by injecting a short-lived radioactive isotope into the system. For a medical scan this usually means injecting the isotope straight into the bloodstream. As the radioisotope decays, it emits positrons. This decay is detectable so the radioisotope is tracked as it moves through the body, producing a three dimensional image that changes over time. This method exposes the patient to some ionizing radiation, although it is a very small amount, around 7 mSv.

2.5 NOISE

All of these methods are highly effective and excellent tools. Their drawbacks are mainly due to the expense of the equipment, the upkeep and the difficulty of use. While a NOISE system could not take the place of these machines, its ease of use and inexpensive equipment could prove a useful alternative in certain situations.

A NOISE image takes only one relatively low powered laser, lenses, and a camera. In total the NOISE system cost \$14,415. The camera, Pixelfly QE High Performance Monochrome Digital Camera, costs \$6,570 (included in total cost). This price includes a PCI card and software to interface with a computer. It is also simple to image an object, there are no large magnetic fields to consider or lead shields necessary. While an X-ray costs a few hundred dollars to develop, this method is simple to develop

since the imaging device is a digital camera and the program to acquire a distinguishable image is relatively short, NOISE can take images cheaply and once the system is bought there is no costly upkeep because the parts do not need to be replenished periodically.

CHAPTER 3

OPTICS BACKGROUND

There are a few optical principles that NOISE uses. It is important to keep the basic scattering model in mind when dealing with NOISE because it illuminates a few key necessities. One is the need for coherent light. Another is the ratio of the scattering coefficient to the absorption coefficient. Both of these issues and the point spread function of this system will be dealt with. The purpose and optical effect that each physical component has will be explained.

3.1 Principles of Scattering

Scattering, a common phenomenon of light occurs when light encounters a medium and a portion of the incident beam is discharged in several different directions. This happens through interaction between incident light and the atoms of the medium encountered. Certain frequencies, or energy packages ($E = h\nu$), are absorbed by specific atoms with corresponding excited states. However, if the light has a lower frequency than these resonance frequencies then the light will not be absorbed. Instead the electron cloud of the atom will start to vibrate around the positively charged nucleus. These oscillations will upset the neutral charge of the atom, creating a dipole which oscillates at the frequency of the incident light. This dipole will give off radiation at the same

frequency. This light is scattered somewhat randomly at the same energy of the incoming beam. The only direction the light will not scatter is along the dipole axis.

If the incoming light is non-coherent it will drive the dipoles at different frequencies causing chaos and the scattering becomes completely random. This makes it impossible to extract any usable information from the resulting image. This is why NOISE needs a coherent light source (a laser) to work.

3.2 Absorption versus Scattering

The NOISE system depends on the relationship between the scattering and absorbing properties of different mediums. Absorption occurs when a photon encounters a medium and the photon and its energy becomes part of the medium. Since NOISE deals with light it is easiest to think in terms of photons. Whether a biological tissue absorbs light depends on the molecules and solid materials in the tissue and the wavelength of the radiation. The energy of atoms or molecules within the tissue consists of four types. These are translational energy, vibrational energy, electronic energy and rotational energy (which only exists in molecules that are not spherical symmetric. The equipartition theorem states that “At thermal equilibrium at temperature T , the average kinetic energy of a molecule per degree of freedom is $\frac{1}{2}kT$.”¹¹ There are two key words in that definition. One is kinetic energy. If other forms of energy in a molecule need to be addressed it is necessary to deal with them separately. The other is average; this theorem can only be applied to a large number of atoms or molecules to be accurate. Often the energy is quantized and we are speaking of discrete energy levels.

When a molecule absorbs energy, it undergoes an energy transition, i.e. a transition from a low energy level to a higher energy level. These transitions fall into three categories, electronic, vibrational, and rotational. Which transitions occur depend on the type of material, the state of the material, the intermolecular bonds involved, the wavelength of light and the crystal structure when applicable. Rotational transitions normally only occur in gasses or fluids. Transitions between energy levels are ruled by selection rules.

Table 3.1: vibrational transitions depending of the molecular bond and elements.⁹

bond	cycles/cm, ν	wavelength, $\lambda = 1/\nu$
C-H stretch	2850-2960 [cm^{-1}]	3.378-3.509 [μm]
C-H bend	1340-1465	6.826-7.462
C-C stretch,bend	700-1250	8.000-14.29
C=C stretch	1620-1680	5.952-6.173
C=C stretch	2100-2260	4.425-4.762
CO_3^{2-}	1410-1450	6.897-7.092
NO_3^-	1350-1420	7.042-7.407
NO_2^-	1230-1250	8.000-8.130
SO_4^{2-}	1080-1130	8.850-9.259
O-H stretch	3590-3650	2.740-2.786
C=O stretch	1640-1780	5.618-6.098
N-H	3200-3500	2.857-3.125

To consider absorption and scattering properties, it is necessary to define a few parameters (see Fig 3.1). First is the absorption coefficient, μ_a (cm^{-1}) which is a measure of the rate of decreasing intensity caused by absorption when an EM wave travels through a medium. It is the fraction of the incident energy that is absorbed per unit length and is given by

$$\mu_a = \rho_a \sigma_a \quad [3.1]$$

where ρ_a (cm^{-3}) is the volume density of the absorber and σ_a (cm^2) is the effective cross-section of the absorber defined by

$$\sigma_a = Q_a A \quad [3.2]$$

' A ' being the surface area encountered and Q_a is a unit-less constant representing the absorption efficiency, in other words the amount of absorption of a certain substance. This "effective" cross-section can be different than the actual size of the absorber.

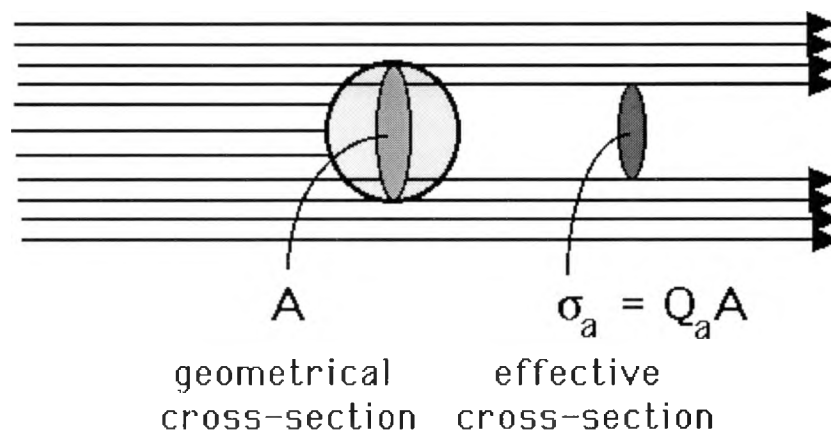


Figure 3.1: geometrical cross section of an absorbing element.¹⁰

The effective cross-section is the size and shape of the light that is blocked by the absorbing agent. This “shadow” is what is recovered by the NOISE process. The probability of survival of the photon after traveling a length L through the material is given by:

$$T_a = e^{-\mu_a L} \quad [3.3]$$

From this equation it is understood that greater the absorption coefficient or the longer the photon has to travel, the more likely it is to be absorbed.

The definition of the scattering coefficient mirrors the absorption coefficient. The scattering coefficient, μ_s (cm^{-1}) is a measure of the rate of decreasing intensity caused by redirection of the photons when an EM wave travels through a medium. It is the fraction of the incident energy that is redirected per unit length and is given by:

$$\mu_s = \rho_s \sigma_s \quad [3.4]$$

where ρ_s is the density of scatter center and σ_s is the effective cross section that is defined by geometrical size and a unit-less constant related to scattering efficiency.

$$\sigma_s = Q_s A \quad [3.5]$$

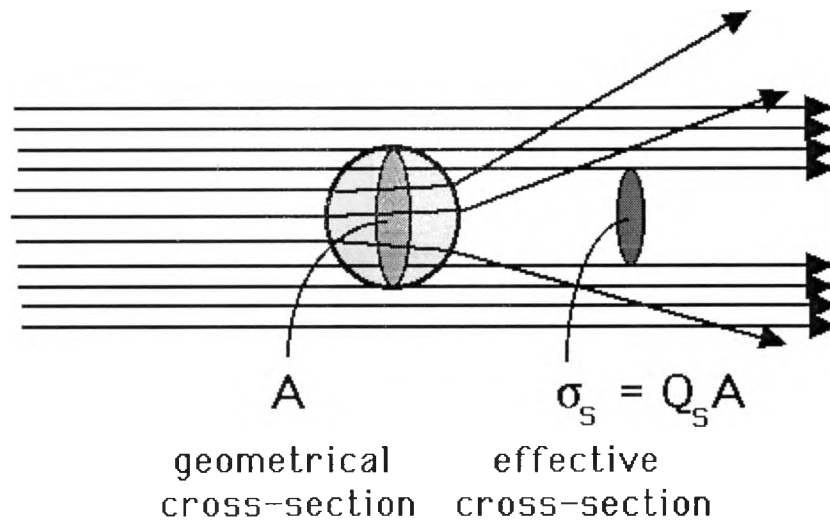


Figure 3.2: geometrical cross section of a scattering element.¹⁰

σ_s describes the amount of scattering due to a specific scattering agent. The probability that a photon is not scattered after traveling a length L through the material is given by:

$$T_s = e^{-\mu_s L} \quad [3.6]$$

The scattering coefficient is usually taken a step further and used to produce the reduced scattering coefficient μ_s'

$$\mu_s' = \mu_s(1 - g) \quad [3.7]$$

where g , the anisotropy factor, is the mean value of the cosine of the scatter angle and is therefore a value between minus one and one. If g is close to 1 the scattering is very anisotropic and more forward scattering than backward scattering will occur. For isotropic scattering g is equal to zero. The anisotropy factor is defined by the following integral:

$$g = \int_{-1}^1 p(\theta) \cos(\theta) 2\pi \sin(\theta) d\theta \quad [3.8]$$

where $p(\theta)$ is the scattering function and describes the probability that a photon is scattered into a unit solid angle oriented at an angle θ relative to the photons original trajectory.

' g ' is the anisotropy factor. In other words, g describes the amount of forward motion a photon has after it has been scattered; or how much it has been deflected from its original path.

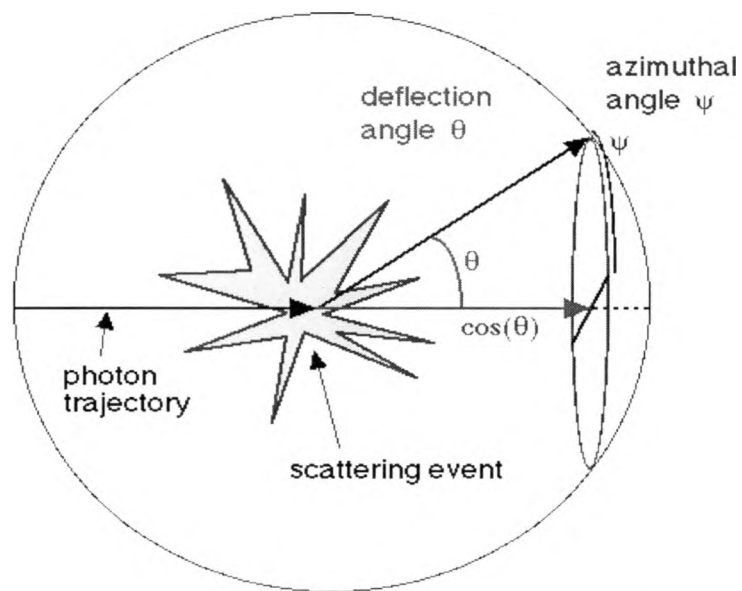


Figure 3.3: several elements of a scattering event.¹⁰

The reduced scattering coefficient not only describes the amount of light that has been scattered, but also how severely it was scattered. In this system, if light scatters too severely it does not encounter the MLA. The diameter of the MLA restricts the severity of the scattering that can be detected.

While all types of scattering are governed by the same physical mechanisms, it is appropriate to use different mathematical models to describe different scattering events. If individual particles are being considered, the Mie theory of scattering is usually applied. Mie's method is used a lot in investigating biological scattering. This theory addresses spherical scatterers of uniform refractive properties, particularly a single refractive index n_p . This theory can be used to approximate many situations; the most common being Rayleigh scattering in the case of very small particles. Calculations using this theory use the surface area of the largest cross-section of the sphere (πa^2) which is the geometrical cross section, and relate it to the effective cross section of scattering, by the scattering efficiency of the sphere.

Mie used Maxwell's equations, in particular;

$$\begin{aligned} \nabla \times \mathbf{H} &= \frac{4\pi\mathbf{I}}{c} + \frac{1}{c} \frac{d\mathbf{D}}{dt} ; \\ \nabla \times \mathbf{E} &= -\frac{1}{c} \frac{d\mathbf{H}}{dt} \end{aligned} \quad [3.9]$$

solving for the boundary conditions. This led a relation to the electric field at the surface of the sphere and the Mie scatter coefficients.

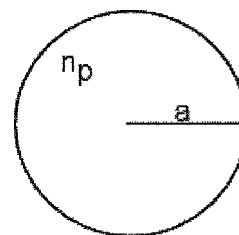


Figure 3.4:
spherical
scatterer of
uniform
refractive index.

$$\begin{bmatrix} E_{sp} \\ E_{ss} \end{bmatrix} = \frac{e^{-ik(r-z)}}{-ikr} \mathbf{S} = \frac{e^{-ik(r-z)}}{-ikr} \begin{bmatrix} S_{11} & S_{12} \\ S_{21} & S_{22} \end{bmatrix} \begin{bmatrix} E_{ip} \\ E_{is} \end{bmatrix} \quad [3.10]$$

E_{ss} (E_{is}) and E_{sp} (E_{ip}) are the electric field perpendicular and parallel to the scatter plane of the scattered (incident) EM wave, \mathbf{S} is the scatter matrix and its elements are the Mie scatter coefficients which are in general a function of the scatter angle θ . Note that

this formulation is very similar to that of the Fresnel reflection coefficients. The factor in front of the scatter matrix; $\frac{e^{-ik(l-z)}}{-ikr}$ is due to the fact that the scattered wave is spherical.

This comes from the actual scatterer being a sphere. At a large distance from the particle (far field), the cross terms of the matrix are zero and the measured intensity becomes:

$$\begin{bmatrix} I_{sp} \\ I_{ss} \end{bmatrix} \sim \begin{bmatrix} |S_{11}|^2 & 0 \\ 0 & |S_{22}|^2 \end{bmatrix} \begin{bmatrix} I_p \\ I_s \end{bmatrix}. \quad [3.11]$$

$|S_{11}|^2$ and $|S_{22}|^2$ are in general a function of the scatter angle and similar to $p(\theta)$, the scattering function. The figure below shows the calculated $p(\theta)$ for the s and p-component of the scattered light for 633 nm large polystyrene particles submerged in water.

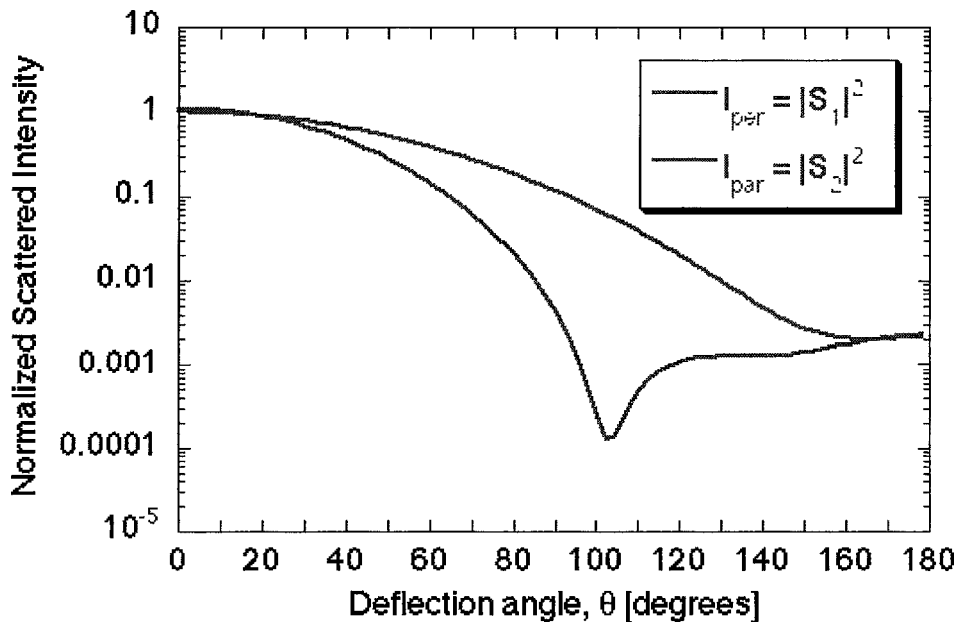


Figure 3.5: Normalized Scattered Intensity as a function of the Deflection angle for a 304 nm diameter polystyrene sphere in water taken with a 633 nm laser.¹⁰

Note that similar that the scatter functions for both polarization directions are not the same and that the p-component has a minimum similar to the Brewster angle for reflection of a plane surface. It is clear that the scattering of this polystyrene sphere is not isotropic. The probability that a photon will scatter forward is much larger than the probability of backward scattering. An isotropic scattering function that scatters light equally in all directions would look like

$$p(\theta) = \frac{1}{4\pi} \quad , \quad \text{such that} \quad \int_0^\pi p(\theta) 2\pi \sin\theta \, d\theta = 1 \quad . \quad [3.12]$$

The Henyey-Greenstein method is another method of scattering calculations. It is used to describe scattering due to clouds of small particles (interstellar dust). Although this method employs many of the same variables it has been found to be a poor approximation of biological scattering due to the fact that it underestimates scattering at large angles¹. This type of scattering though might become important when we will try to use NOISE to increase the visibility in dust-storms (military applications) or smoke (fire-fighter application).

Table 3.2: scattering and absorption coefficients of various biological tissue.⁶

Tissue	λ , nm	μ_a , cm^{-1}	μ_s , cm^{-1}	μ_s , cm^{-1}	g	preparation
Epidermis	800	40	420	62	0.85	Frozen sections
Dermis	800	2.3	175	30	0.85	Bloodless tissue Hydration 85%
Lung	635	8.1	324	81	0.75	Frozen sections
Uterus	635	0.35	394	122	0.69	Frozen sections
Aorta	633	0.52	316	41.0	0.87	Freshly excised, kept in saline
Liver	635	2.3	33	100	0.68	Frozen sections
Female breast: Fatty normal	836	0.11	7.27			Excised, kept in saline, 37°C
Female Breast: Benign tumor	625	0.33		3.8		
Esophagus	633	0.4		12		2.5 mm slab
Prostate	850	0.6	100		.94	Shock frozen sections Of 60-500 μm , .5-3 hrs post mortem
Forearm	800	.23		6.8		Time-domain technique $\mu_s \approx 16-7.9 \cdot 10^{-3} \lambda$, $\lambda=500-1060$ nm
Calf	800	.17		9.4		$\mu_s \approx 16-7.9 \cdot 10^{-3} \lambda$, $\lambda=500-1060$ nm

3.3 Point Spread Function and Symmetry

A point spread function (psf) is the path that light travels from the source to the camera where the image is taken. Mapping the psf of this optical system contains some oddities. Certain parts of the path are easily dealt with. The lenses used have well defined optical properties that have been thoroughly explored. Their effects can be taken separately from the more complicated elements. The psf of the object itself is also simple. Either light encounters the object and is blocked by it or the light is not affected by it. It is considered a binary object because it outputs one of two outcomes. Mathematically it is easy to define as a function that gives a zero if the light encounters the objects position and a one if it does not. The scattering layers are more difficult to define. Mathematically they are considered random scatterers, but their position and thickness determine how they affect the image.

One thing to notice about the psf of the system is that it is theoretically asymmetric. Symmetry means that if a photon enters the system at a certain point traveling along a specific path, travels through the system and then exits at a specific point in a specific direction it is possible send a photon through the system at the exit point moving in the exact opposite direction and it will come out at the entrance point moving in the exact opposite direction as the original photon did after traveling along the same path.

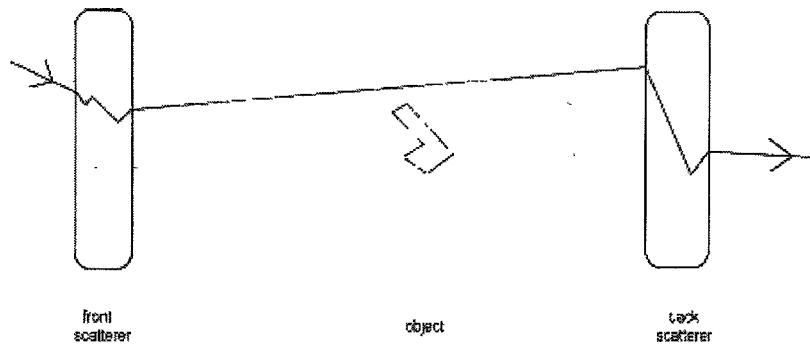


Figure 3.6: light path through front and back scatterers.

In a symmetric system, light takes the same path in one direction as it does moving in the opposite direction. Most optics systems are symmetric (lenses, mirrors.)

In actuality, if a single photons path through each specific cell is considered, it is possible to trace a path that is symmetric. Taking the psf of each cell, separately they are all symmetric.

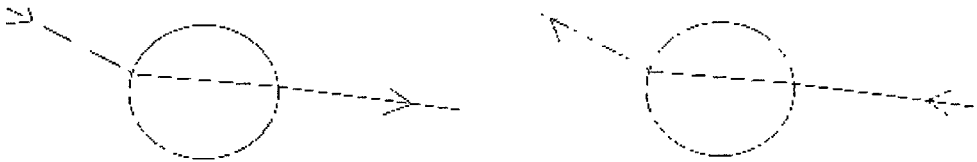


Figure 3.7: symmetric light path through a cell.

This approximation of the system can only be used if the scattering is not considered random, and while it is a valid approximation, possibly more valid than the one that used here, it is not useful for NOISE. NOISE exists on the principle that the scattering is completely random. This is also a good approximation because the content and width of the scattering medium is not mapped, so when the scattering medium is considered as a whole, its scattering properties are random. This is beneficial, especially

for the medical aspects of the method, because it would be difficult if not impossible to map a person's body and the invasiveness of that procedure would negate any advantages of the NOISE method.

What makes the system asymmetric is the randomness of the scattering. If the scattering is considered random two identical photons moving along identical can enter the system at the same point yet come out at different points moving in different directions. Technically this interpretation of scattering is not correct; unless the medium changes, identical inputs will always give identical outputs. For the purposes of NOISE this interpretation is incorrect. Taking this into account means several things. One is that the back scattering acts completely different than front scattering. This will be explained later in this chapter. It also means that taking an image from one side of the system will not give the same picture as taking the image from the opposite side. This factor is important to consider in medical situations because it might be extremely beneficial to take an image from a certain direction depending on what the picture is being taken of and where the object is embedded.

It is important to note that the array of images has no symmetry. This is a more obvious observation, but it is good to understand that NOISE only works when the speckle patterns are different from each other. Any kind of symmetry within the array would cut down on the useful amount of images to go into the averaging algorithm. Due to the irregularity of the scattering there is no discernable pattern including symmetries of any kind to the images.

3.4 Scattering Effects Due to Each Component

Geometrically, the scattering of the two layers is different. The front scatterer and the back scatterer, although identical in make-up, have different effects on the system.

The first layer of chicken randomly scatters incoming light. Incoming parallel light is provided by a laser. This front scatter layer acts as a diffuser for the binary object. Without the front scatter layer it will be difficult to image the binary object. All light that encounters the object is absorbed by the object, effectively creating a silhouette. At this point the light encounters the second piece of chicken and is randomly scattered again. This backscatter layer will diffuse the image of the object.

The distance between the first scatterer and the object (a) and the second scatterer and the object (b) are effectively dealing with the position of the object.

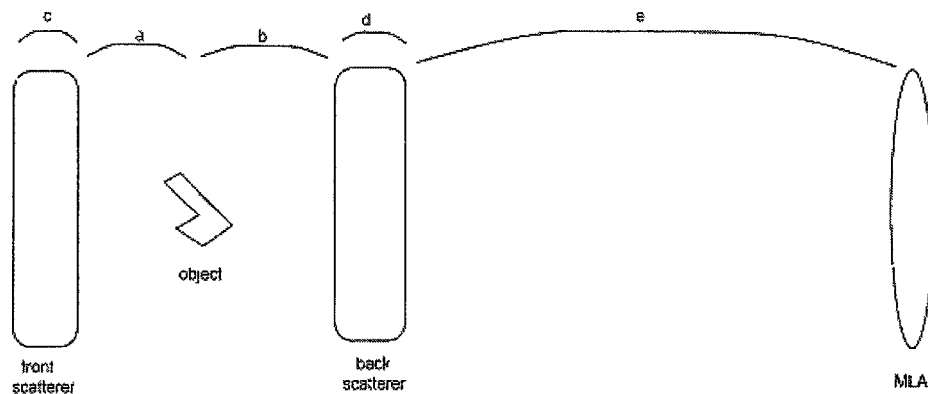


Figure 3.8: elements of the NOISE system.

First, what happens if b is kept to a short distance (3 cm) and 'a' is set to about 4 or 5 times that? As 'a' increases, the light rays that are scattered at more extreme angles

exit the system, leaving light beams that are close to parallel. In addition, the short b distance prevents the light scattered at shallower angles from traveling far and blurring the silhouette. As the thickness of the front scatterer, ' c ', increases the object becomes more defined in the image. Increasing the thickness of ' c ' also decreases the intensity as more light is absorbed into the front scatterer. Also, the larger the system gets, the more light is lost to scattering, lowering the intensity of the final image and obscuring the object.

If ' a ' is kept short and b is lengthened a completely different effect takes place. Drastically scattered light still escapes the system. After the light is scattered by the first layer of chicken and encounters the object, creating a silhouette, it continues along its path and the scattering angles become more and more evident. The end product is extremely blurred. As a result of this, it is preferable to keep b to a reasonably short distance.

As a and b approach zero the scattering angle remains the same but the light is not allowed to travel as far on their vectors so the scattering is drastically reduced.

The widths of the two chicken pieces have different effects. The width of the first piece of chicken increases the amount of the scattering angles and increases the randomness of the scattering. Although the layers of chicken are considered to be completely random scattering agents, an extremely thin slice of chicken does not effectively scatter light. As the width increases the light is scattered multiple times as it encounters each layer of chicken. Another effect is that more light is absorbed by the chicken.

The width of the second piece of chicken has similar results. The thicker the slice is, the more light is absorbed and the scattering becomes more drastic.

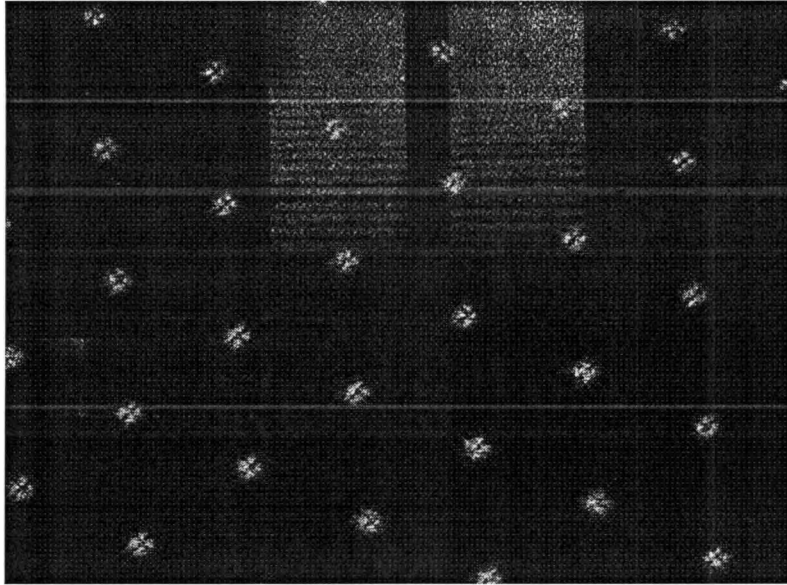


Figure 3.9: cross with back scattering, illumination provided by red laser.

CHAPTER 4

NOISE SYSTEM

While building my system, there were several constraints to work with. One was minimizing the floor plan of the setup. Dr. Rosen et al. constructed a system that had a surface area of approximately 32 square feet. This setup had 4 square feet to work with. The total length of this setup was 787.5 mm compared to 1385 mm for the Rosen-group setup. It also works without a large lens that Rosen group had. This restricted the field of view when working with the MLA, which led to complications. What follows is a description of the theory behind the physical aspects of the NOISE system and how they were used them to build my own system.

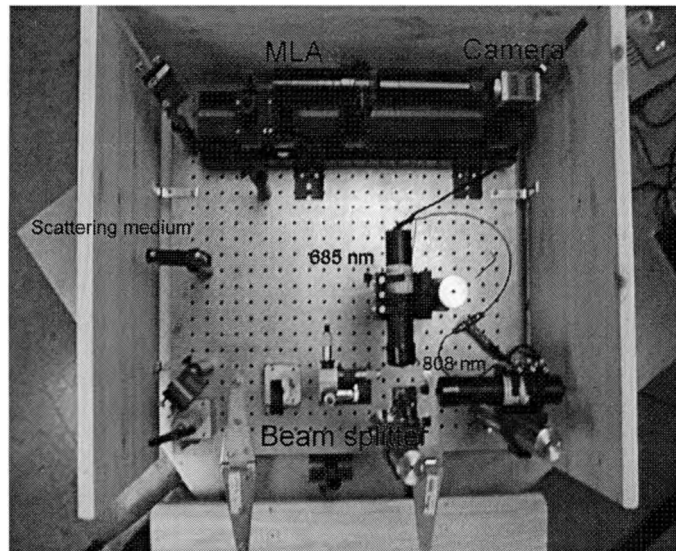


Figure 4.1: floor plan of setup.

4.1 System Specifications and Theory

Some of the parameters of this system are given as constants. The focal length of the MLA is one of them. Others are variable, specifically the distance between the MLA, camera and object. Some of the considerations when assigning these distances are the image to object ratio and the amount of lenses in the MLA that will be useful. If the object has length L , it can be placed on the optical axis giving a length $L/2$ and $-L/2$ above and below the axis.

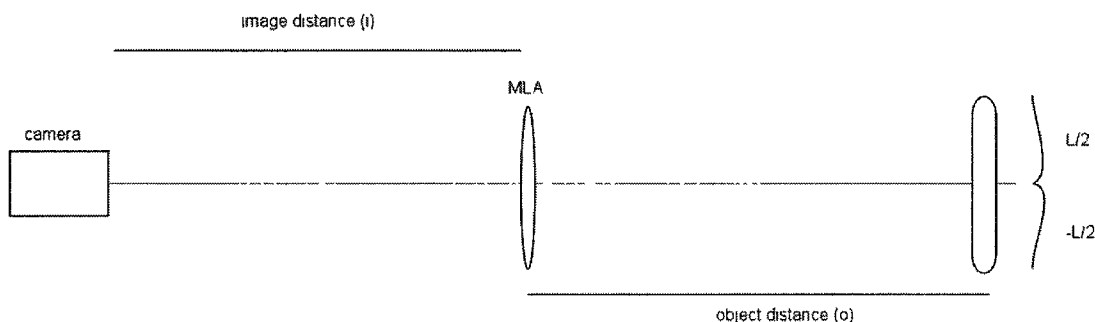


Figure 4.2: object, image distance.

Since this object is going to be a biological object, it will not be possible to adjust its size. If the object is too large, adjacent lenses in the MLA will give overlapping images. There are several ways to adjust this. Increasing the object distance works, or placing a lens between the MLA and the object which would decrease its height. The height should be decreased to half of the diameter of the MLA lens. This would make the magnification

$$m = \frac{D/2}{L/2} = \frac{D}{L} \ll 1, \quad [4.1]$$

$$\text{and since } m = \frac{i}{o} \ll 1, \quad [4.2]$$

the object distance will be much greater than the image distance. So for $i \ll o$;

$$\frac{1}{i} + \frac{1}{o} = \frac{1}{f} \quad [4.3]$$

$$\frac{1}{o} + \frac{1}{m \cdot o} = \frac{1}{f}; \text{ because } m = \frac{i}{o}$$

$$\frac{1}{i} + \frac{m}{i} = \frac{1}{f}$$

$$\frac{1}{i}(1+m) = \frac{1}{f}$$

$$\frac{i}{1+m} = f; \text{ m is small so } 1+m \approx 1$$

$$i \approx f$$

So making a few substitutions

$$m = \frac{D}{L} = \frac{f}{o}; \text{ or}$$

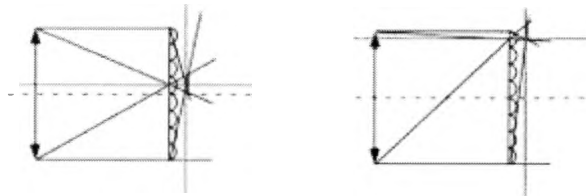
$$o = \frac{f \cdot L}{D} \quad [4.4]$$

So if the focal length of the MLA is fixed (about 3mm or 3000 μ m), the diameter of the lens is known and the

object distance is fixed the

maximum size of an object that

can be imaged is $L = \frac{o \cdot D}{f}$. [4.5]



Since the object will be

biological and its size will not be adjustable the system has to make adjustments accordingly. A lens between the MLA

Figure 4.3: ray diagram of the field of view of the MLA.

and the object works well with the image from the lens being the object for the MLA. A diaphragm in front of the MLA puts a definite limit on the size of the object, preventing the images from the MLA to overlap. This also cuts down on stray light coming into the system. After the MLA another lens magnifies the images and selects the center 10 by 10 images of the MLA. The lens selects images by magnifying the overall image from the MLA so that the only the 10 by 10 images are incident on the camera. The camera's detector is 1.114 mm long, so the magnification of this lens

$$m = \frac{C}{10 \cdot D} = \frac{11.14 \text{ mm}}{10 \cdot (0.5 \text{ mm})} = 2.28 .$$

After the number of images is calculated it is

beneficial to block the images that are not used from the camera. This cuts down on stray light and improves the contrast of the final image. To do this, a diaphragm should be placed after the MLA. This diaphragm should be placed 3mm after the MLA which is right after the image distance for the MLA.

4.2 Multi-Lens- Array Concerns

A multi-lens array (MLA) is an array of a few hundred small lenses connected together. These are made by a laser lithography technique. A lens is etched so there is an array of bumps all of the same size on the lens. The lens is then heated and the bumps liquefy, forming half-spheres held together by surface tension. When these droplets solidify they become an array of uniform lenses.

Each of the lenses in the MLA has a diameter of 500 microns. This small diameter is necessary so that each lens only catches light that is scattered at the same angle.

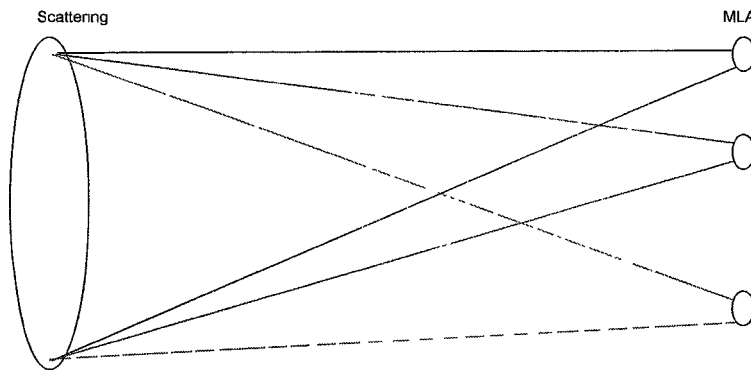


Figure 4.4: each lens of the MLA captures a different bit of scattered.

NOISE takes many speckle images of the same object all from different angles so each image has caught different parts of the light that has been scattered.

By taking pictures with the MLA without any scattering mediums we were able to determine the problems inherent in using a MLA. One such problem is the difference in images captured by the center lenses of the MLA and the lenses on the edge, called “edge effects.” The MLA was positioned so that the object was centered in the lens in the middle. As the lenses got further from the center, the object shifted to the outside edge of each lens, so the field of view captured by the center lens is not the same as the outer images.

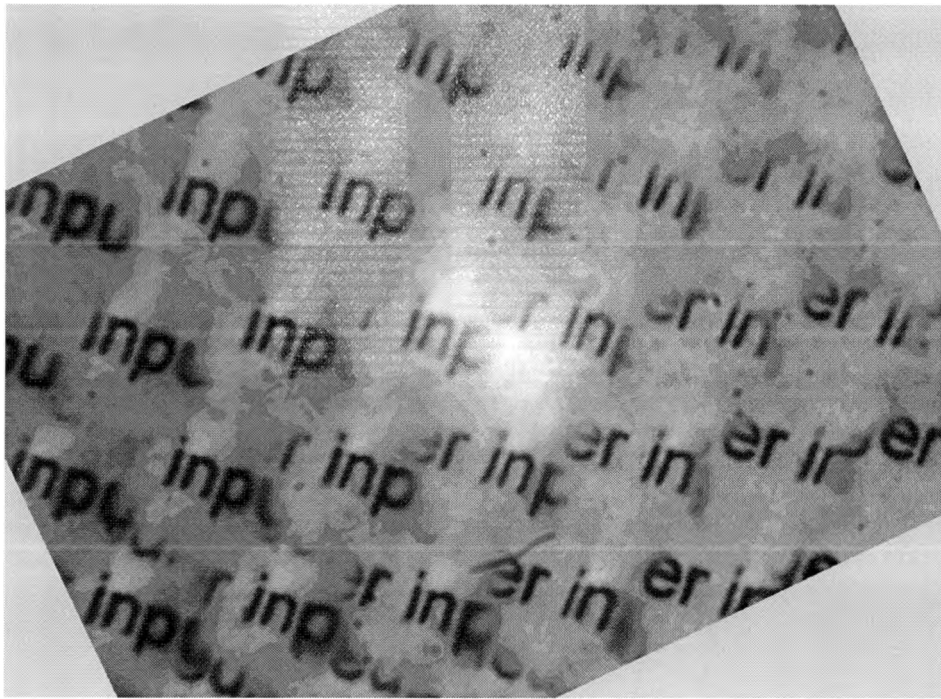


Figure 4.5: picture taken with the MLA without scattering.

From this picture it is obvious that there is a shift in what light reaches each separate lens. On the right the lens captured the letters "er" while on the left "inp" was imaged. Another problem that associated with this technique is the shifting focus. While the center lens was focused on the image the outer lenses tended to blur and pick up less light, making them darker and fuzzier in respect to the center.

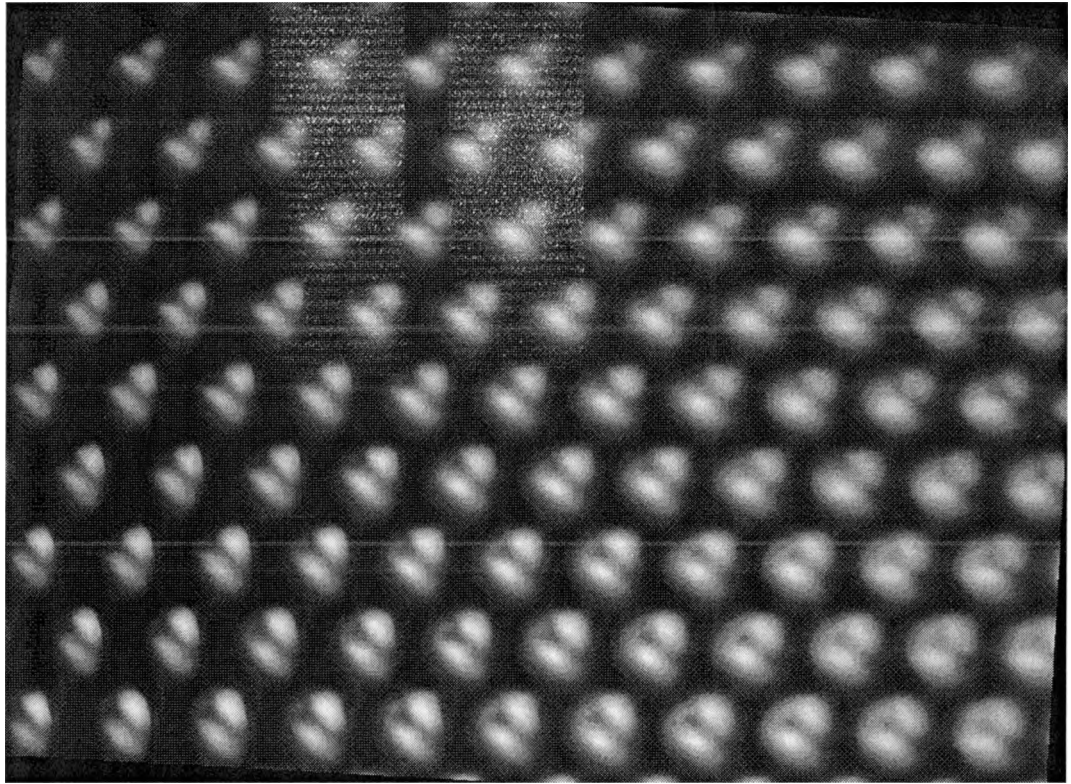


Figure 4.6: picture of object embedded in chicken while being agitated.

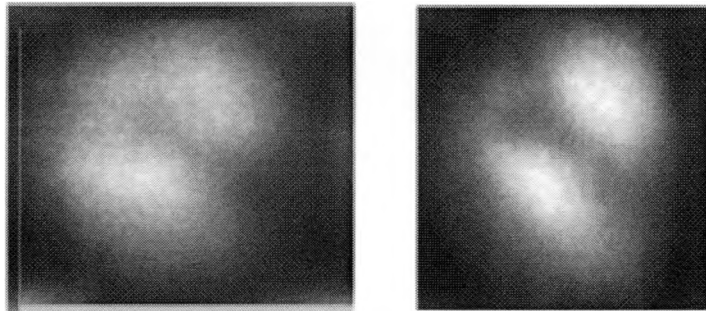


Figure 4.7: image on the left is taken from the outer edge of the array; image on right is taken from the center of the array. Notice the image on the right has more definition than the one on the left.

As a side note, an interesting phenomenon occurs when an image is taken of an object embedded in chicken while the chicken is being agitated. The speckles are severely reduced or even disappear, leaving a much clearer image of the object. This is because the camera is set to take pictures at a slower rate than the chicken is moving so the speckles are blurred giving a more defined image.

Although the object was embedded in chicken breast, the picture taken by the center lens is less blurred than one taken by an outer lens. The smaller the angle between the object and the MLA the less edge effects occur. However, while it is desirable to keep the object shift to a minimum, the scattering angle needs to be as varied as possible. The goal of NOISE is to capture light scattered at different angles, imaging different speckle patterns. The difference in the speckle patterns is the key to acquiring a complete representation of the object. So there is a balance to be struck between maximizing the scattering angle and minimizing the edge effects. There are several ways to deal with this problem. One is to take select only the center images to be averaged. With the NOISE1 program it is possible to select which group of images to be averaged and how many are going to be used. Another way to deal with this problem is to lengthen the distance between the object and the MLA. Since one of the objectives in this project was to minimize the setup's length, instead of lengthening the distance we installed a negative lens between the MLA and the object. The disadvantage of this is that the image was minimized, leaving less detail. Due to the nature of the system though, this does not reduce the clarity of the picture. This is because any image obtained with this system is a blurry silhouette. The blurriness can be minimized but any image obtained will not have interior detail.

4.3 System Configuration

When light moves from one medium to another it is reflected, absorbed or transmitted. Which one of these happens depends on the refractive index of the mediums, the angle of incidence and the wavelength of the light. For the purposes of this project the incoming light is perpendicular to the medium so the angle of incidence is always 90° .

The system here consists of a laser (with several different wavelengths whose advantages will be discussed later), the MLA, a highly sensitive camera and a series of lenses.

The MLA is designed with a hexagon structure. It contains a more than 500 lenses, each of them 500 microns long with a focal length of 3.3 mm.

The camera is a PixelFly QE high performance monochrome digital camera system. This camera contains a monochrome scientific grade 0 CCD chip with 1390 times 1024 pixels. The CCD is 2/3" format which means that the size of the CCD chip is 6.6 mm by 8 mm (diagonal is 11 mm). The pixels are squares and have a size of $6.45 \times 6.45 \mu\text{m}^2$. The readout time of the CCD is 79.8 msec which will result in 12 frames per seconds at full resolution. This will enable the setup to be used to study processes in real-time. The integration time of the camera can be changed from 0.01 msec to 10 sec via the interface. The camera head contains a 12 bit AD converter that converts the light

intensity collected by each pixel in a 12 bit digital number. These digitized values are sent as 2 byte words to the PCI card in the back of the computer.

The camera has a C-mount to which a lens can be attached. A C-mount is a 1 inch diameter female fitting with a thread of 32 TPI (threadings per inch). A microscope objective or a lens can be attached to this fitting. The distance between the CCD chip and the shoulder of the mounting ring is 17.5 mm. This distance is sometimes called the back focal length. In this setup the camera is directly connected to a C-mount tube system that contains the MLA, the lenses, and the diaphragms.

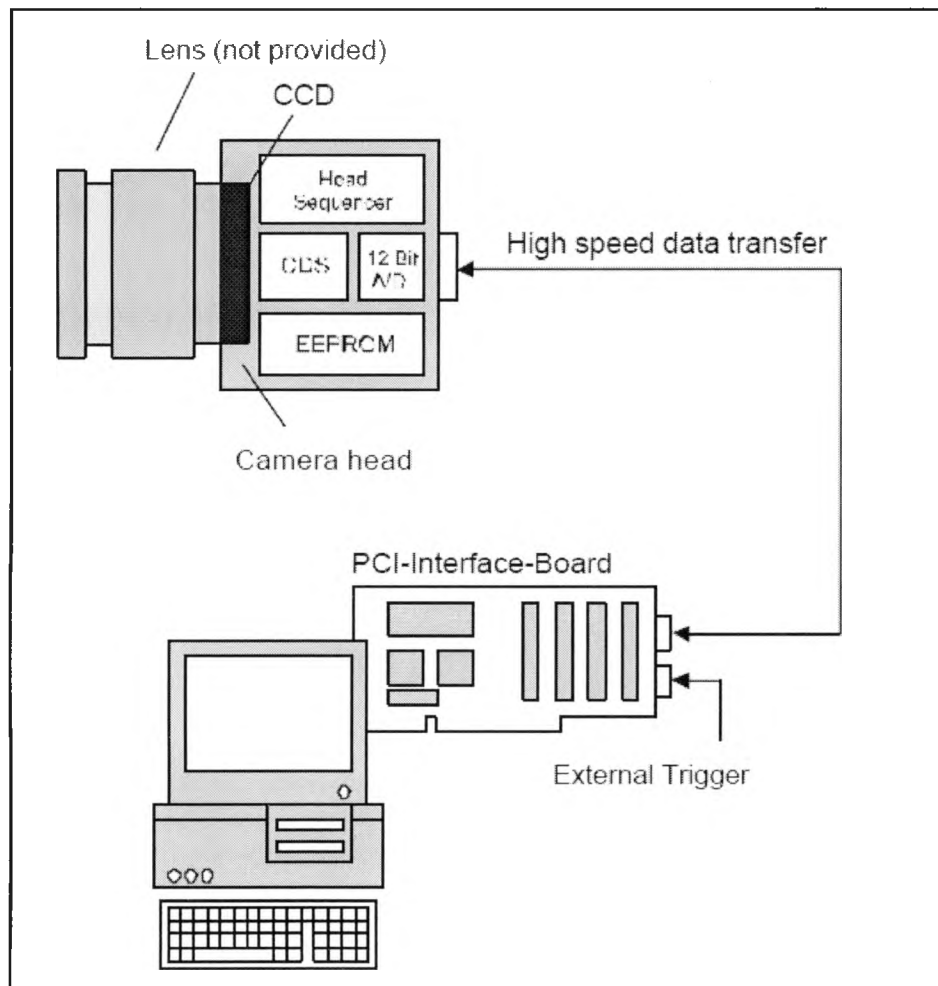


Figure 4.8: configuration of the camera connection to the computer.

This system was tested with several different scattering mediums including frosted glass, paper and chicken meat (breast meat). Several different setups were explored. Each one had advantages and disadvantages. These mainly had to deal with the MLA. If the entire MLA was imaged the edge effects became extreme and were difficult to deal with. At the same time, it was possible to take more channels with this image

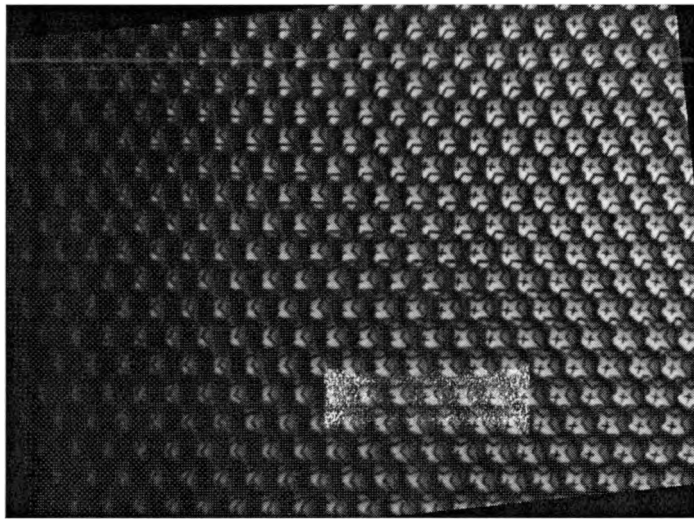


Figure 4.9: image that maximizes the number of channels but has visible edge effects.

From this image, it is possible to see that although there are almost 100 channels, only the ones in the top right quarter are usable. Another setup only looked at the center 12-16 channels. While all of these channels were usable, this drastically constricted the number of images that could be summed to reduce the scattering effect.

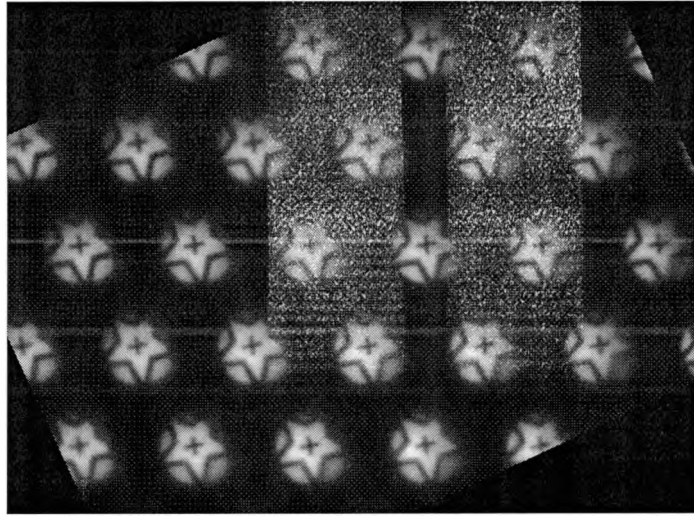


Figure 4.10: image that reduces edge effects; however this severely limits the number of channels.

The final setup was a compromise between the two, 40-50 usable channels.

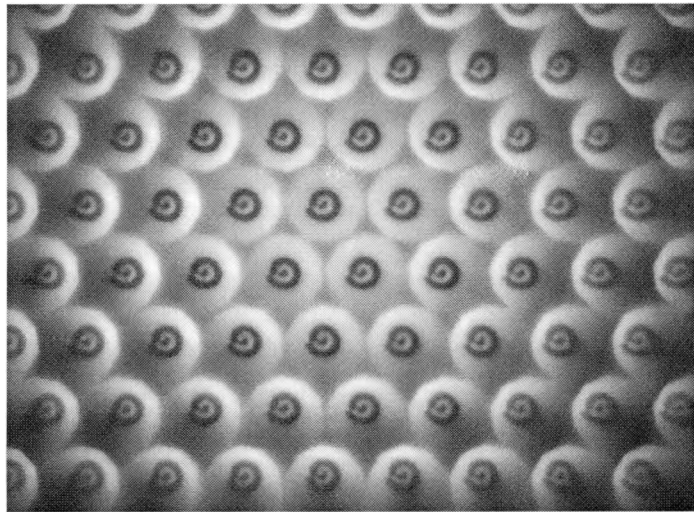
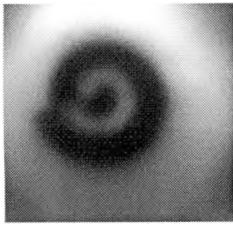


Figure 4.11: final setup; maximizes usable channels while minimizing edge effects.

Each channel clearly displays the object and has a uniform focus. The light variation on the outer edges averages out.



This image was achieved with a total length of 787.5 mm between the object and the camera.

Figure 4.12: summed picture of above array.

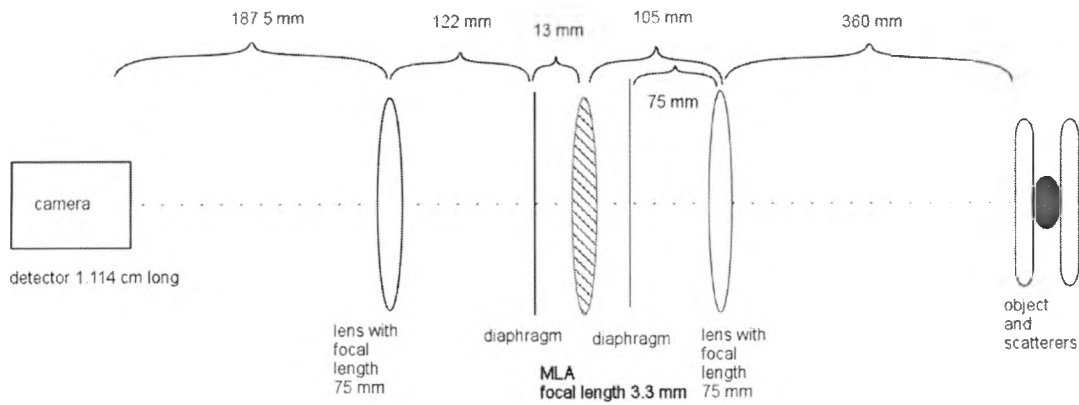


Figure 4.13: system design

CHAPTER 5

BIOLOGY

NOISE in the near infrared specifically targets the near infrared region because biological tissue is especially transparent in that region. This is not to say it is completely transparent, just more transparent than in other regions. To test this information, the optical properties of the sample chicken were measured using the FTIR setup and the filmetrics setup. Because cell structure plays a large part in the scattering of light there is a simple explanation of a cell included, and its various organelles that are responsible for the scattering.

5.1 Cells

Cells are generally broken up into two categories, prokaryotic and eukaryotic. The simplest type of cell is prokaryotic. All the chemicals and enzymes that are needed to produce energy, growth and division are contained in the cytoplasm. The DNA is attached to the plasma membrane so there is no nucleus. This type of cell does not exist in living animals; they only exist as single celled organisms such as bacteria or algae.

Eukaryotic cells make up living animals. These cells are more evolved than prokaryotic cells. They have nuclei and internal organization. Their internal structure involves many organelles that each has a specific purpose. The nucleus is the largest

organelle. It is the planning organism of the cell. Inside the nucleus is the nucleolus which helps make RNA. It also contains DNA, the code by which genes are programmed. The nucleus walls or 'membrane' are permeable. This membrane is double walled and the permeability is caused by sub-microscopic holes in it. Protein can flow into the nucleus from the cytoplasm through these holes and RNA can flow out of the nucleus back to the cytoplasm. Cytoplasm describes the fluid (cytosol), organelles and other inclusions inside the cell. Cells reproduce by the nucleus splitting into two distinct nuclei.

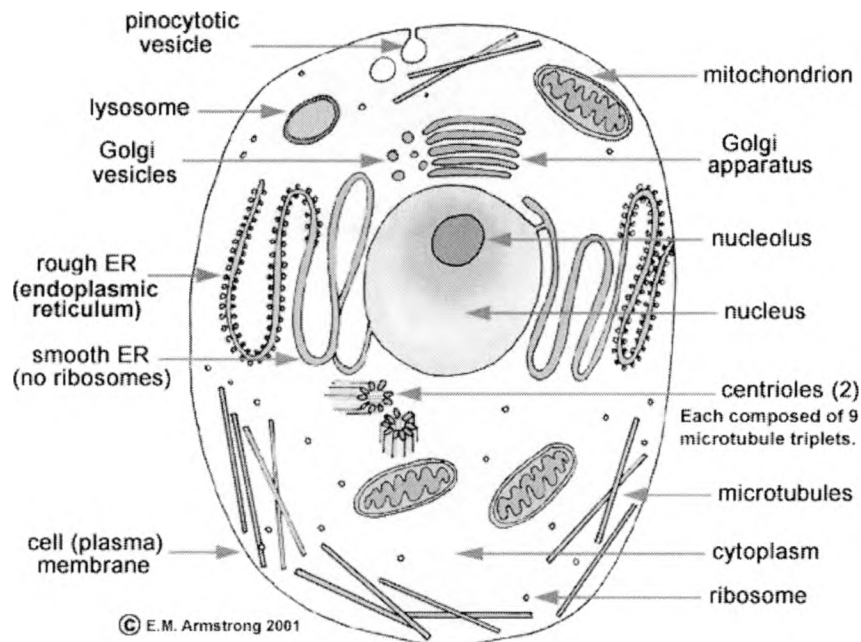


Figure 5.1: diagram of a cell.⁸

Mitochondria are an organelle that produces energy within a cell. Mitochondria have a double membrane that has a lot of surface area but not a lot of volume. It is draped into many folds so it does not take up a lot of space. It captures enzymes in the folds and uses them to turn the sugars and fats in the cytoplasm into energy. Mitochondria are unique; they are the only organelle in a cell that reproduce themselves.

This means that they contain their own DNA instead of their DNA being stored in the nucleus.

There is a membrane system in the cell, called the endoplasmic reticulum. It separates the molecules that are leaving the cell from the molecules that are used in the cell. It also helps synthesize the larger molecules that make up the other organelles. There are two types of endoplasmic reticulum, smooth and rough. The smooth is made mostly of small hollow tubes. This type is more prevalent in cells that process lipids. The rough is more prevalent in cells that make a large amount of protein. It has a flattened, sac-shaped interior and has ribosomes attached to its outer surface.

Ribosomes are small spheres that lie on the endoplasmic reticulum. They are made of RNA and protein.

The Golgi apparatus is a stack of membranes that are all connected with spaces between them. They are part of the final processing of newly made proteins. The Golgi apparatus make two organelles, lysosomes and peroxisomes. The lysosomes are used for digestion inside the cell and the peroxisomes detoxify the cells, breaking down any toxic substances that build up inside cells.

The entire cell is surrounded by a membrane. This membrane allows certain substances in and out of the cell. It also stops substances that should not enter or leave the cells.

All those organelles have a slightly different refraction index (see table 5.1). Most of the organelles in the cell have a very low absorption coefficient.

These structures and their small changes of the refraction indices are what are responsible for the scattering through biological material. This means that every time

light encounter a different cell organelle, the light is scattered again, leading sometimes to multiple scatterings within a single cell.

5.2 Biological Effects on Scattering

The medical application of this technique demand consideration of the optical properties of biological tissue, specifically the scattering properties of cells.

The first thing to consider is the optimal wavelength of light to use. The more light that goes through the scattering medium, the more information is available, so a wavelength that has a small absorbing coefficient (or a large scattering coefficient) is best. Previous studies have thoroughly mapped the optical properties of biological tissue. What has been found is a “therapeutic window” where the absorption of the light is minimal. In this wavelength range more light is scattered than absorbed.

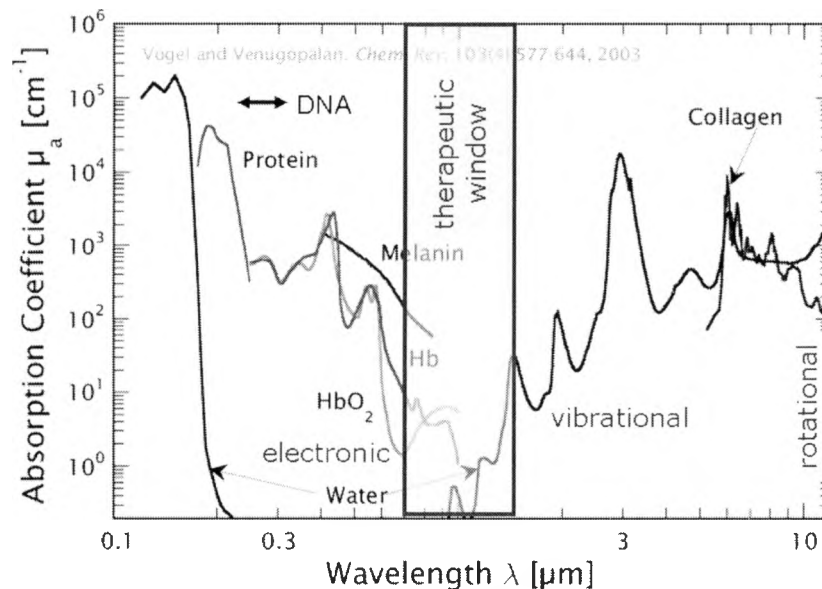


Figure 5.2: the therapeutic window exists where the absorption coefficient is minimized with respect to wavelength.¹⁵

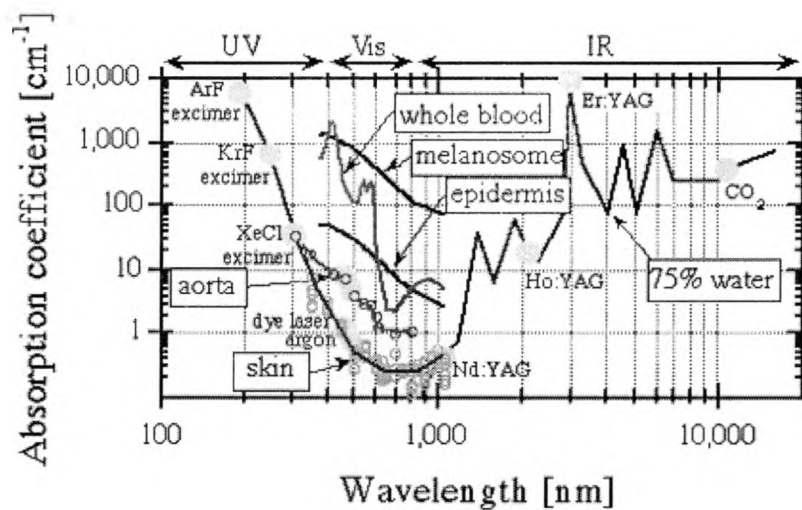


Figure 5.3: absorption coefficients of various biological structures with respect to wavelength.¹⁰

This window is between 650 and 1500 nm; on the short wavelength side of this window the light is absorbed by blood while on the long wavelength side water is the main absorber. This wavelength range is called the near-infrared (NIR). The near-infrared (N-IR) is where most measurements of scattering are taken since that will obtain the most information. In this window the absorption coefficient is about 0.3cm^{-1} which gives a penetration depth of 3cm. We used an 808 nm wavelength for measurements.

The scattering of biological cells can be attributed to a few things. One is the size of the cell and another is its contents. The different structures of a cell each have a different refractive index. Biological tissue is an inhomogeneous material. Not only do the different types of cells of different shapes, sizes and properties, the cells themselves are made up of a variety of materials. Most of the scattering through a mammalian cell is due to the internal structures of that cell¹. This means that the shape of the cell does not have a great effect on the scattering.

Table 5.1: refractive indices of various cellular structures.

Index of refraction values	
Cell component	Refractive index
Surrounding medium	1.35
Cytoplasm	1.37
Cell membrane	1.46
Nucleus	1.39
Melanin	1.7

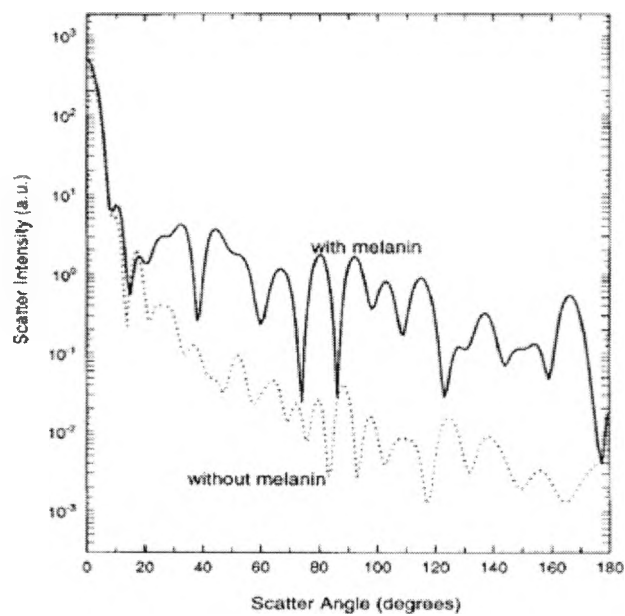


Figure 5.4: scatter intensity with respect to the scatter angle. Notice that melanin has a higher scattered intensity.²

One thing to notice is that melanin has a higher index of refraction than the rest of the cell. Since melanin can be varied in the same type of cells, it could be beneficial in considering what area of a body to image if the choice is applicable.

Variations in the internal structures have a large effect of the scattering of each of the cells. The scattering increases with the size of the nucleus. The intensity of light scattered from a cell with no nucleus is about 250 a.u. more than a cell with a normal sized nucleus taken at a scattering angle of 0° . A cell with a large nucleus is about 150 a.u. less than the normal sized nucleus' scattering at 0° . The curves of all three of these cells' scattering versus scattering angle all exhibit the same characteristics, roughly Gaussian, decreasing as the scattering angle increases.

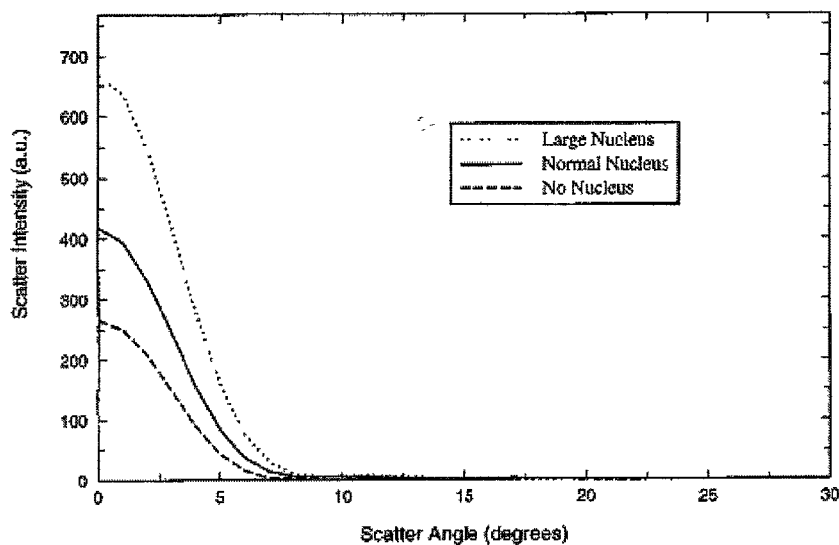


Figure 5.5: as the size of the nucleus increases so does the scattered intensity.²

Interior organelles also have an effect on scattering. Although at angles close to zero the curves are very similar, albeit the cells with organelles have smaller peaks; the two curves show less and less similarity as the angle increases (See Fig 5.6.) Since the intensity of the scattered radiation at these angles is so small the difference between the

patterns could be considered negligible. What should be considered is even when the two curves diverge so much in peaks and patterns the cell without organelles always has a higher intensity than the cell with organelles at the same angle.

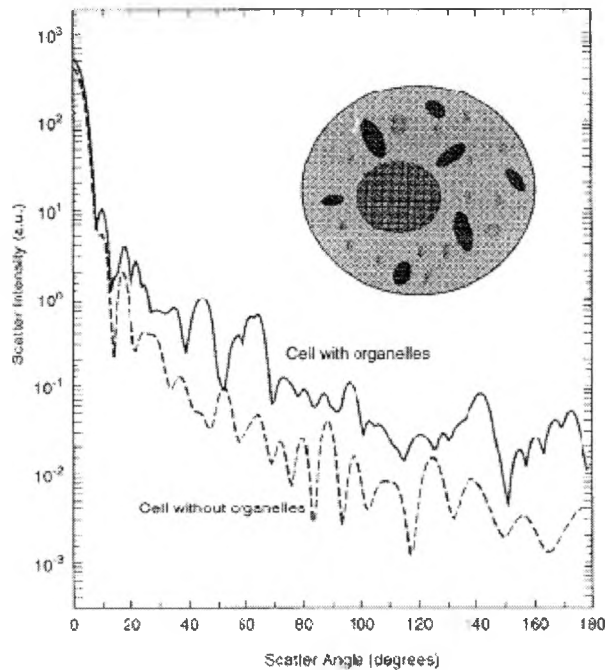


Figure 5.6: scattering of a cell with and without organelles.²

There are a few differences between cancerous cell and healthy ones, including extra chromosomes, higher protein concentration and changes in nuclear shape and texture. These all lead to a different refractive index, making cancer cells optically different than normal cells. Cancerous cells usually have

a higher nuclear to cytoplasmic ratio³, changing their refractive index. It might

be possible to exploit these differences using speckle images to detect the difference between sick and healthy cells.

5.3 Analysis of Chicken

The NOISE system exploits the optical properties of chicken, in particular the relationship between scattered and absorbed light. NOISE works with monochromatic

light so the interaction between light and chicken meat was mapped based on wavelength, looking a maximum of scattering. Two types of analysis were performed, FTIR and filmetrics. For all of these measurements, small, thin slices of meat were taken so that they were as homogeneous as possible.

FTIR (Fourier Transfer Infrared Spectroscopy) has several different measurement modes and sample holders. The two modes attempted were transmission mode and frustrated total internal reflection mode. The latter mode was ruled out after taking measurements. This mode sets up an evanescent wave in the sample. However its measurement depth is very small. The chicken used was fresh, so it had a layer of liquid on its surface. While taking measurements in this mode optical properties similar to water were observed and it was concluded that the evanescent wave was not penetrating the meat but the thin layer of liquid surrounding it. This gave information about the liquid but did not map the actual meat. The transmission mode was more successful. This mode takes measurements of intensity after light has passed through the sample. This mode forces the light to interact with the entire sample instead of just the surface. The light source ranged from the visible to the near infrared. After taking a background reading without the sample, the chicken was placed directly in the light path, and another reading was taken, which was displayed as the percentage of the intensity of the background reading versus wavelength. A 2mm thick sample of lean turkey was used for this measurement. This data becomes unreliable for wavelength less than 750 nm due to limitations of the detector, although the data still has a reasonable low deviation. From past studies it was expected to find a maximum around 800 nm (in the N-IR range). The maximum found was a slightly higher (≈ 880 nm) but still in the N-IR range.

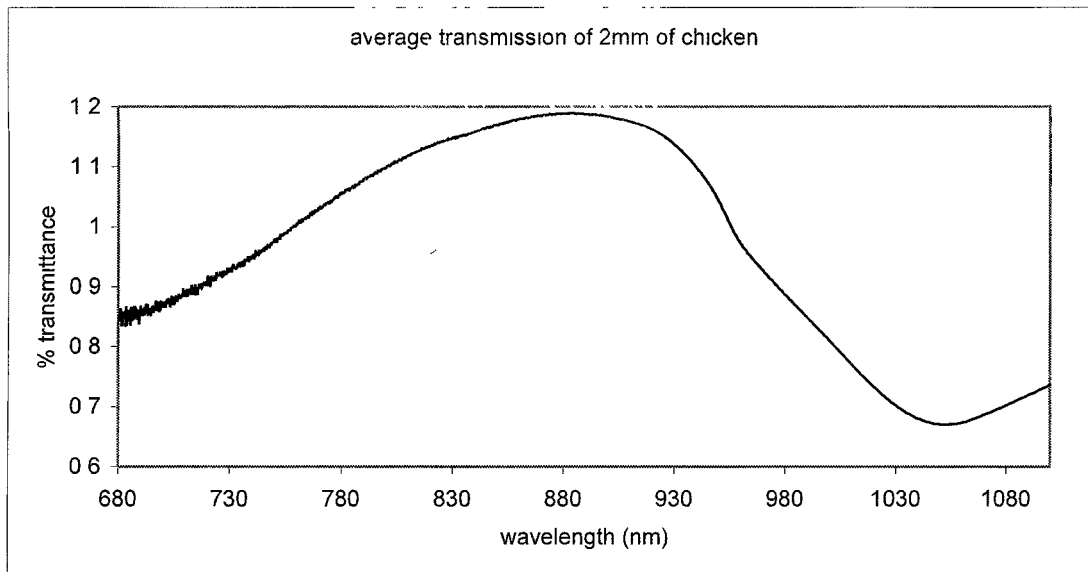


Figure 5.7: transmission with respect to wavelength of 2mm of chicken.

The other type of measurement used was filmetrics. This also used a transmission type of measurement. For this measurement the sample had to be placed on a microscope slide whose optical properties had to be accounted for. Several measurements were taken using different thicknesses of chicken.

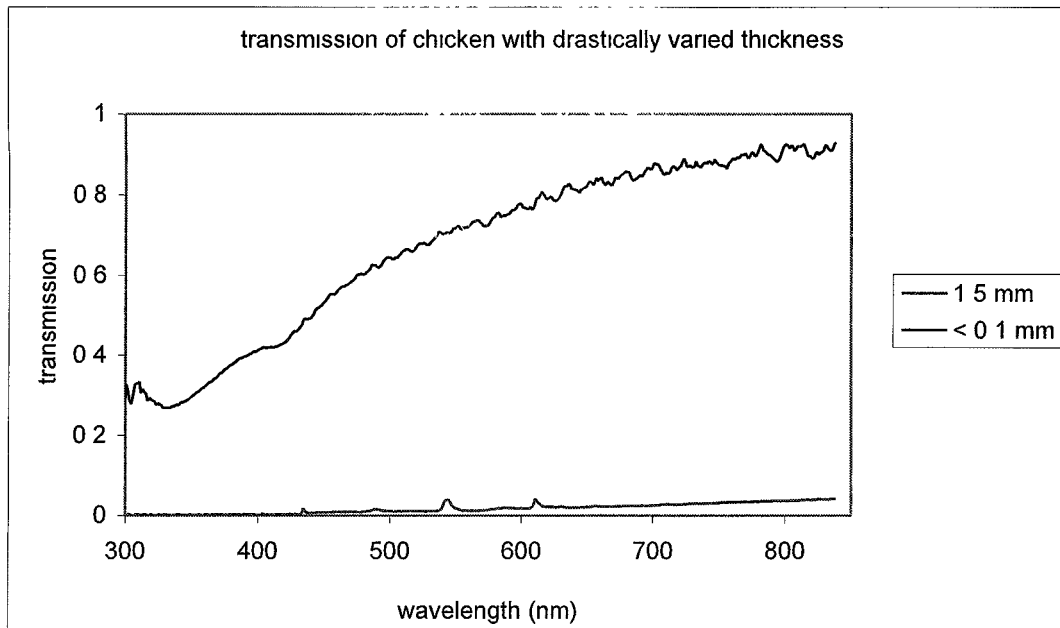


Figure 5.8: as thickness of the chicken increased the overall transmitted light decreased. There is still a clear trend with respect to wavelength.

The thickness of the chicken affected the intensity of the readings but did not change the overall pattern.

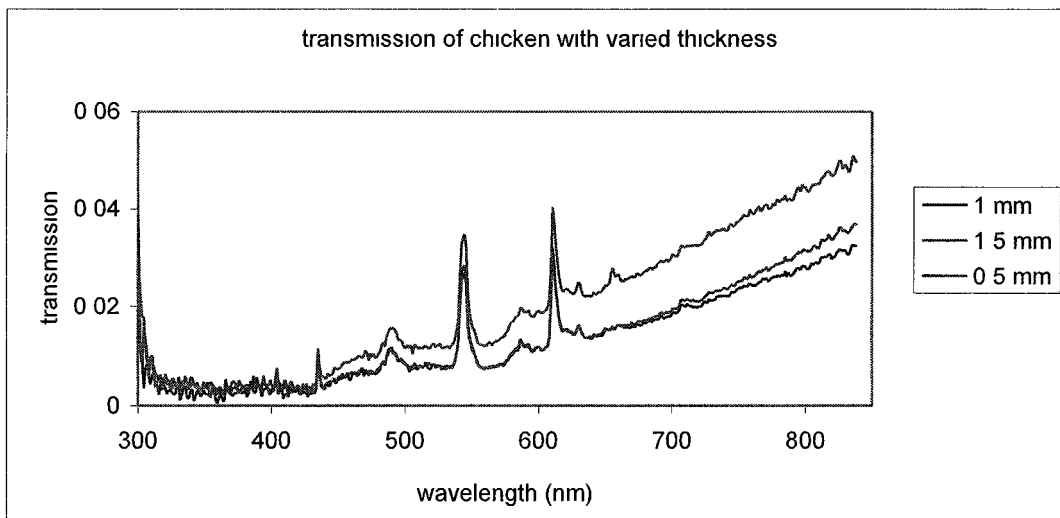


Figure 5.9: effect of small variations in thickness on transmission.

Another variable is the content of the chicken. Being a biological substance, it is not uniform. Several measurements were taken of the same thickness but in areas of the chicken consisting of different elements (fat, tendon, muscle). The general pattern still existed in all of these elements; the difference was in the amount that was transmitted (See Fig. 5.9).

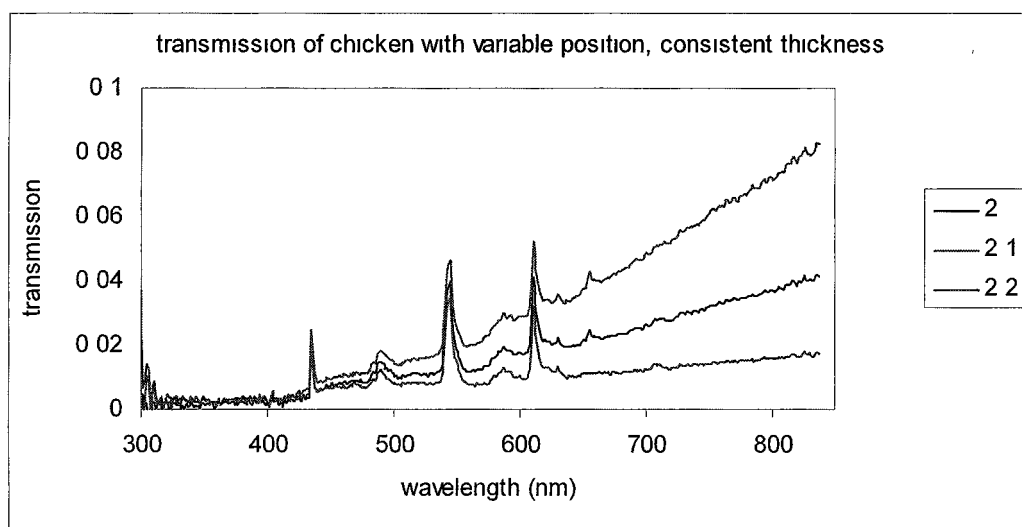


Figure 5.10: these measurements were taken with different types of chicken tissue (fat, muscle).

The spikes in these measurements are due to the source used and at wavelengths less than 350 nm the deviation in measurements becomes too large for these measurements to be useful. In the higher wavelengths the slope of this data matches up nicely with the FTIR measurements.

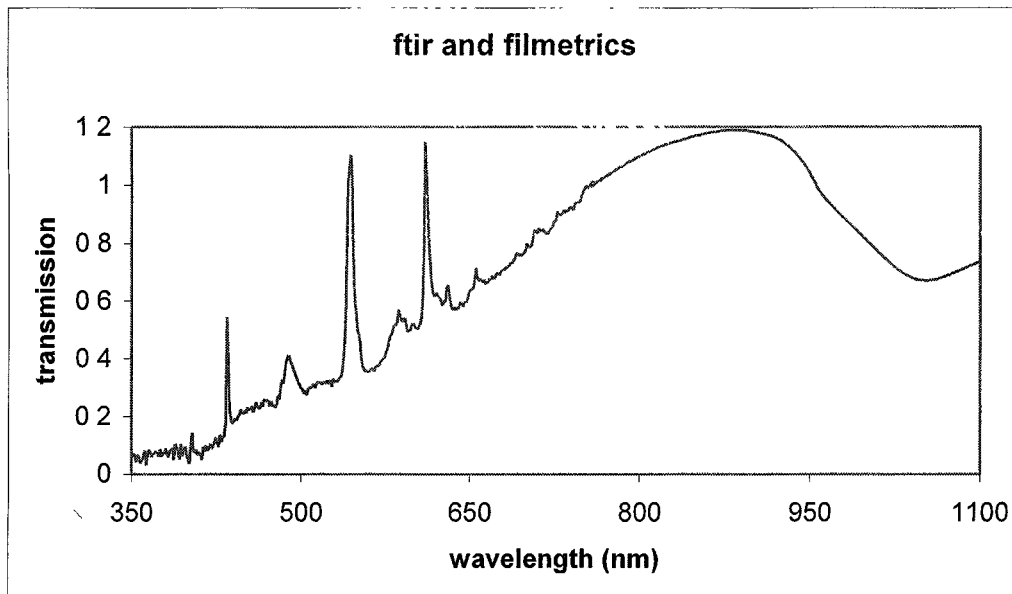


Figure 5.11: ftir and filmetrics data.

Since the overall trend of both graphs matches as well as behaving similarly to earlier studies, it was concluded that the chicken samples used here are similar to ones used by Dr. Rosen. This also indicates that chicken meat is a good indicator of other biological tissue.

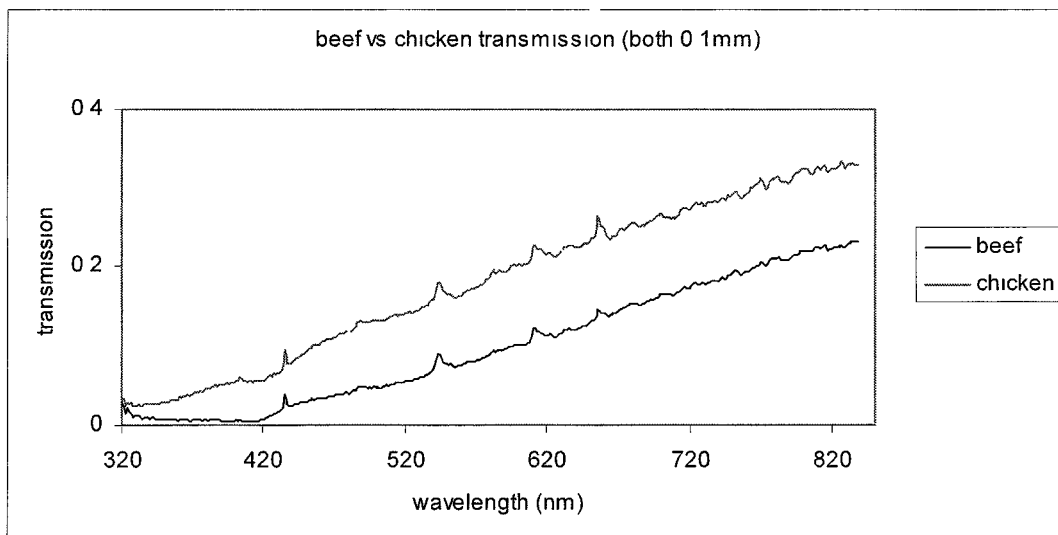


Figure 5.12: transmission of beef versus chicken.

Several readings of a beef sample to confirm this. While the beef absorbed more light than chicken of similar thickness, they both absorbed less in higher wavelengths than lower.

Some of these measurements were done with chicken breast and some were performed with lean turkey.

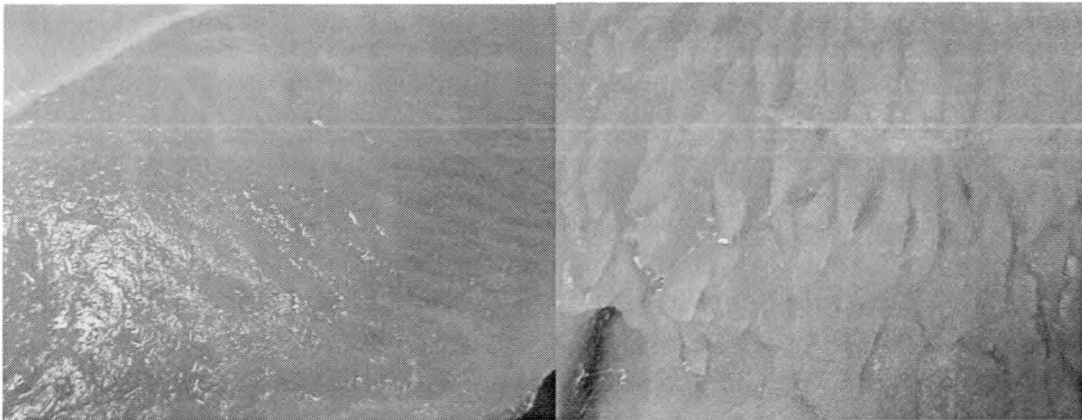


Figure 5.13: left is chicken breast; right is lean turkey; both are raw. Note that the textures are different.

While the optical properties of these meats were extremely similar (the only differences seemed due the unavoidable differences in the thicknesses), the turkey did not seem appropriate for the NOISE system. This is because of the texture of the meat. The chicken's surface is very smooth while the turkey is segmented. In small slices, the texture, being a macroscopic phenomenon, does not affect the optical properties of the turkey. With a larger amount of turkey it did cause irregularities in the intensity of the image because some light had to travel through more meat than other, leading to greater absorption.

CHAPTER 6

PROGRAMMING

After constructing an optimal setup and obtaining an image of an object embedded in a scattering medium an image has to be extracted. The image that has been taken is a speckle image and unrecognizable as an image of the object. The main concept is to stack these images on top of each other and add them. There are several methods to do this. One is a 'shift and add' algorithm. Another is an image registration technique. With this technique the addition is still necessary but the shift is unnecessary.

2.1 Shift and Add

The first NOISE program that was written to average the images together is a simple shift and add algorithm. This program takes preset lengths, extracts each image according to these lengths and adds them on top of each other. One of the issues to deal with is the grid lengths made by the MLA. This is important because the lengths specify where one image ends and the next one begins. If the lengths are not correct then the position of the object's image will shift. If the two images are not lying exactly on top of each other then the image will become fuzzy show up as a blob.

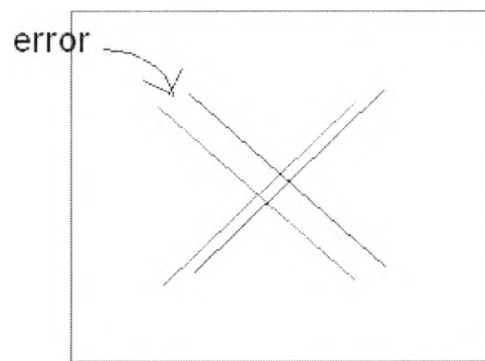


Figure 6.1: the difference between the two x's will produce a fuzzy final image.

To determine the grid lengths, NOISE1 has a user calibration routine that has the user set the grid lengths by selecting a rectangle that is twice as large as a single cell. The routine takes the average length to set the length and height.

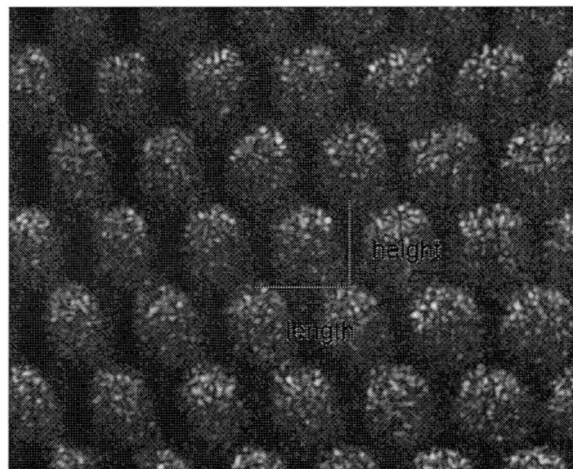


Figure 6.2: height and length of one channel; image taken with scattering.

From Fig. 6.2; the separation of the cells is not obvious even when each cell is distinct. It is necessary to take a picture without any scattering to get a good approximation of the lengths.

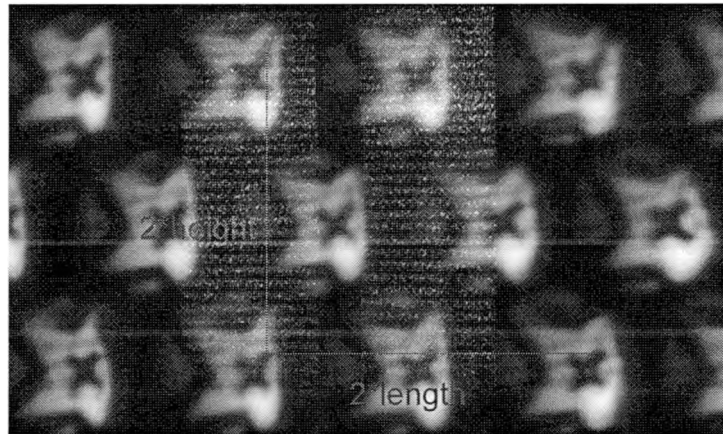


Figure 6.3: image taken without scattering for calibration.

By picking out a point on a distinct image the user is able to calibrate the grid lengths accurately. It is only necessary to change this calibration if the MLA is moved in relation to the camera, or if any lenses are changed in between the two. After the grid lengths are set, the user sets which cell to start the process. From this starting point NOISE1 extracts a cell then shifts in the x direction by the length of the cell, adding each cell to the previous as it goes. After the length of a row, which the user controls, NOISE1 shifts up one row and repeats the adding process. It is also necessary to shift over half the length of a cell since the array shifts at each row. This is because of the “bricking” of the array, each adjacent row is shifted by one-half of the length of the cell. NOISE1 continues to shift and add in this manner until it has reached the number of rows that the user specified. This program will automatically adapt these specifications if the user indicated to add more rows or columns than exist in the array. When the program is finished it will display how many images were added together and the final image.

6.2 Isomorphisms and Frequency Space

NOISE1 does not affectively deal with edge effects, especially the difference in the images caught by the center lens and the outer lenses. NOISE2.1 deals with this problem using an image registration technique. NOISE2.1 is similar to the NOISE2 program written by the Rosen group but has a few differences that have to do with the specific image registration technique used. Image registration is a way to locate shapes within a picture. There are several registration techniques, the two methods used are a cross-correlation and the absolute difference. A cross-correlation looks like

$$h(X) = \int_{-\infty}^{\infty} f(x+X)f^*(x)dx \quad [6.1]$$

in the space domain, where $f(x+X)$ represents the shape (template) that we are looking for and $f^*(x)$ is the complex conjugate of the original image. A cross-correlation compares an image with itself. The “ $x+X$ ” is the amount that the image is shifted with respect to itself. There are a few simplifications that can be made to this. One is to notice that $f(x) = f^*(x)$ since the intensity is always going to be real. This makes the cross-correlation look more like a convolution.

$$h(X) = \int_{-\infty}^{\infty} f(x+X)f(x)dx \quad [6.2]$$

$$\text{Compared with a convolution: } h(X) = \int_{-\infty}^{\infty} f(x)g(X-x)dx \quad [6.3]$$

The few differences between these operations can be resolved by letting the function $f(x+X)$ be the same as the function $g(X-x)$ and realizing that the addition or subtraction of ‘ x ’ simply refers to the images shift with respect to each other and as long

as the integration covers the entire space between them it does not matter which one is used. At this point the cross-correlation can be expressed as a convolution between a function and itself. This entire operation can be translated to the frequency domain by performing a fourier transform on both images. The operation then looks like

$$\mathfrak{F}[f(x)] \cdot \mathfrak{F}[g(x)]. \quad [6.4]$$

This product will be at a maximum when the shape in $g(x)$ (the template) is lying directly on top of the corresponding shape in $f(x)$ (the image). NOISE2.1 puts the template over the image and takes the cross-correlation, then shifts $g(x)$ over pixel by pixel taking the cross-correlation at each point and then returns the position of $g(x)$ when the cross-correlation is at a maximum. After NOISE2.1 has registered where each image is (there should be as many images as cells in the array) it averages them, recovering a usable image.

The absolute difference (NOISE3) is similar. Instead of taking the product of the two functions, it takes the absolute difference. When the shape in $f(x)$ and $g(x)$ line up; the difference should be zero. Because the image has been scattered there is not an exact match so instead of looking for a zero, the minimum absolute value of the difference is taken.

To move between position space and frequency space, it is necessary that all operations done in frequency space are preserved when switching back to position space and vice-versa. This is the convolution property of fourier transforms. To prove this it is necessary to show a one to one and onto correspondence between the two.

Homomorphism: for some

$$F(k) \text{ and } G(k) \in \text{frequency-space} \ni F(k) = \int_{-\infty}^{\infty} f(x)e^{ikx} dx \text{ and } G(k) = \int_{-\infty}^{\infty} g(x)e^{ikx} dx \quad [6.5a,b]$$

where $f(x)$ and $g(x) \in \text{position-space}$

$$G(k) - F(k) = \mathfrak{F}[f(x) - g(x)]$$

$$\mathfrak{F}[f(x)] - \mathfrak{F}[g(x)]$$

$$\int_{-\infty}^{\infty} f(x)e^{ikx} dx - \int_{-\infty}^{\infty} g(x)e^{ikx} dx$$

$$\int_{-\infty}^{\infty} (f(x) - g(x))e^{ikx} dx$$

$$\mathfrak{F}[f(x) - g(x)] \quad [6.6]$$

So the operation is preserved, this operation is homomorphic.

1-1:

let $F(k)$ and $G(k) \in \text{frequency domain} \ni F(k) = G(k)$

$$F(k) = G(k)$$

$$\int_{-\infty}^{\infty} f(x)e^{ikx} dx = \int_{-\infty}^{\infty} g(x)e^{ikx} dx$$

$$\frac{d}{dx} \left[\int_{-\infty}^{\infty} f(x)e^{ikx} dx = \int_{-\infty}^{\infty} g(x)e^{ikx} dx \right]$$

$$f(x)e^{ikx} = g(x)e^{ikx}$$

$$(f(x)e^{ikx}) = g(x)e^{ikx} e^{-ikx}$$

$$f(x) = g(x)$$

Onto:

for every $F(k)$ in frequency-space \ni an $f(x)$ in position-space

$$F(k) = \int_{-\infty}^{\infty} f(x)e^{ikx} dx \quad [6.5a]$$

$$\frac{d}{dx} \left[F(k) = \int_{-\infty}^{\infty} f(x)e^{ikx} dx \right]$$

$$\frac{d}{dx} (F(k)) = f(x)e^{ikx}$$

$$\frac{d}{dx} (F(k))e^{-ikx} = f(x)$$

So the transformation is onto.

$$F(k) \cdot G(k) = \mathfrak{T}[f(x) \otimes g(x)] \quad [6.6]$$

$$\text{let some function } h(X) = f(x) \otimes g(x) \quad [6.7]$$

$$\begin{aligned} \mathfrak{T}[f \otimes g] &= \int_{-\infty}^{\infty} h(X)e^{ikX} dX \\ &= \int_{-\infty}^{\infty} e^{ikX} \left(\int_{-\infty}^{\infty} f(x)g(X-x) dx \right) dX \\ &= \int_{-\infty}^{\infty} \int_{-\infty}^{\infty} e^{ikX} f(x)g(X-x) dx dX \\ &= \int_{-\infty}^{\infty} \left[\int_{-\infty}^{\infty} g(X-x)e^{ikX} dX \right] f(x) dx \end{aligned}$$

this is possible because $f(x)$ does not depend on X , and e^{ikX} does not depend on x

$$\text{setting } (X-x) = w$$

$$dX = dw$$

$$\begin{aligned}
&= \int_{-\infty}^{\infty} \left[\int_{-\infty}^{\infty} g(w) e^{ikw} e^{ikx} dw \right] f(x) dx \\
&= \int_{-\infty}^{\infty} f(x) e^{ikx} dx \int_{-\infty}^{\infty} g(w) e^{ikw} dw \\
&= F(k) \cdot G(k)
\end{aligned}$$

So $F(k) \cdot G(k) = \mathfrak{F}[f(x) \otimes g(x)]$ holds and multiplication in fourier-space is isomorphic to fourier transform convolution of functions in position-space. It is possible to look at the convolution instead of the autocorrelation because of the simplifications made above.

These isomorphisms show that it is possible to perform operations in the frequency domain or the space domain without loss of information. Performing simple operations (multiplication or subtraction) in the frequency domain is faster than performing an equivalent operation in the space domain. This is because an image's information can be compressed in the frequency domain compared to the space domain. Compressing images usually results in a loss of information. This is not a concern because for the purposes of these programs, the compressed images are only used for image registration. After the positions of the object are taken that image is extracted from the original image, not the one that has been transformed.

This registration technique compensates for the difference in position of the objects images in each cell of the array. It does not help the images that are darkened or blurred by edge effects. For the purposes of NOISE the multiplicative operation (convolution) is better than the absolute difference method because it gives a higher, more defined peak. For these reasons only the multiplicative version was written.

6.3 Program Specifics

Two programs were used to take pictures, Camware and a Labview driver provided by the Cooke Corporation. Camware was primarily used due to its easy user interface and adjustable setting. Images were taken with these programs and then we used our programs to extract usable data from them. All the programs were written in Labview version 7.1.

After an image is captured it is in an array format. For the shift and add program to work the lengths of each square has to be found. The array is not a square array, it is a hexagonal lattice.

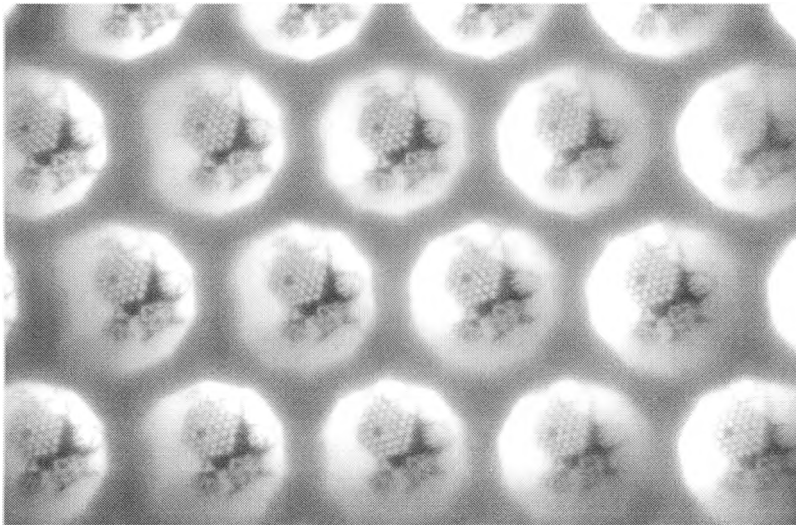


Figure 6.4: bobcat imaged through the MLA without scattering. The slight edges that are visible in each channel are due to the diaphragm in front of the MLA.

For this program it can be considered a square array because the each entire hexagon is not being added, just the image in the middle of it.

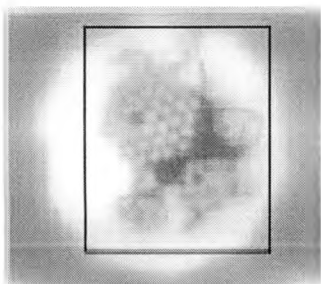


Figure 6.5: the image inside the hexagon can be contained in a rectangle.

What is being found is the exact distance between each image

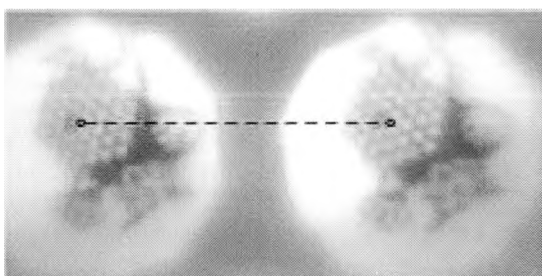


Figure 6.6: grid length.

To do this the image must be indicated (file pathname) before the program starts. This can be done by clicking the folder icon beside the 'photo array to be averaged' and selecting which image to be used. This image has to be taken without any scattering. The 'black bitmap' that is referred to needs to contain the file of a bitmap of the same size of the array with every pixel set to zero (black).

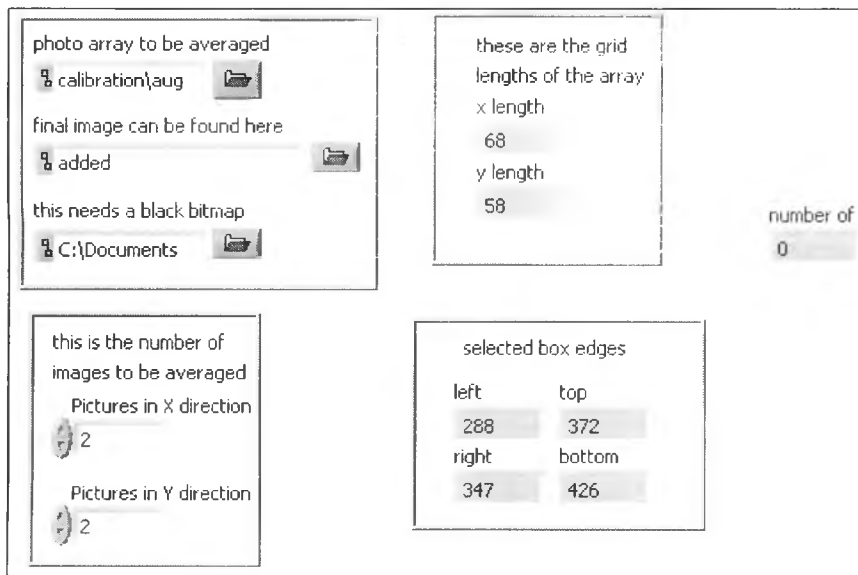


Figure 6.7: user interface for the grid calibration program.

The program will display the image and prompt the user to select a rectangle where the top, left corner is situated on a distinct feature of the object, the top right corner is in the same feature two channels to the right, and the bottom left corner is on the same feature two channels down.

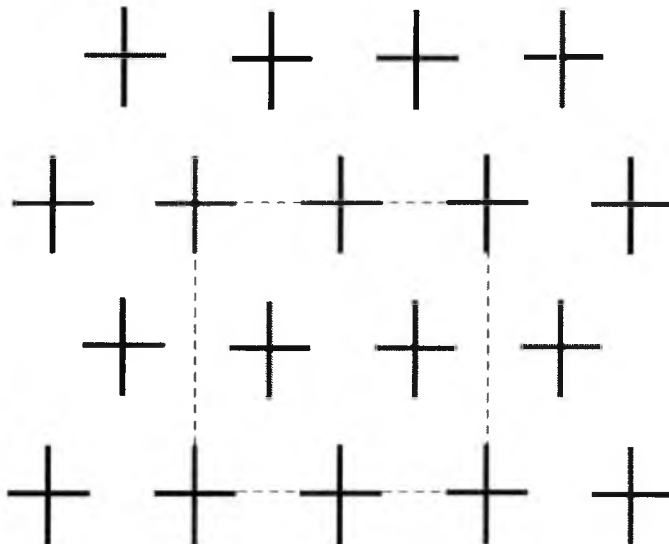


Figure 6.8: the corners of the rectangle all lie on the same feature of the object.

The program will take the lengths of the square, divide them by two and display them under 'these are the grid length if the array; x length; y length'. It should be noted that these are not perfect squares, x does not equal y. These lengths are in pixels. The program then performs the shift and add algorithm, displaying the end product.

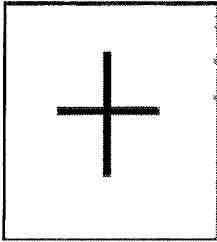


Figure 6.9:
summed image.

Since this image does not have any scattering the end product should be as clear as the original array. If it is not, then the calibration is not a good one and the user should run the program again being more careful about selecting the rectangle. Sometimes it is helpful to use a different feature on the image. Using this program we were able to calibrate the grid down to the pixel.

The grid changes every time the MLA or any lens between the MLA and the camera are shifted. Every time the grid changes it is necessary to recalibrate.

Once the grid is calibrated, the x and y lengths need to be inputted into NOISE1 under 'Calibration Values; x length; y length'.

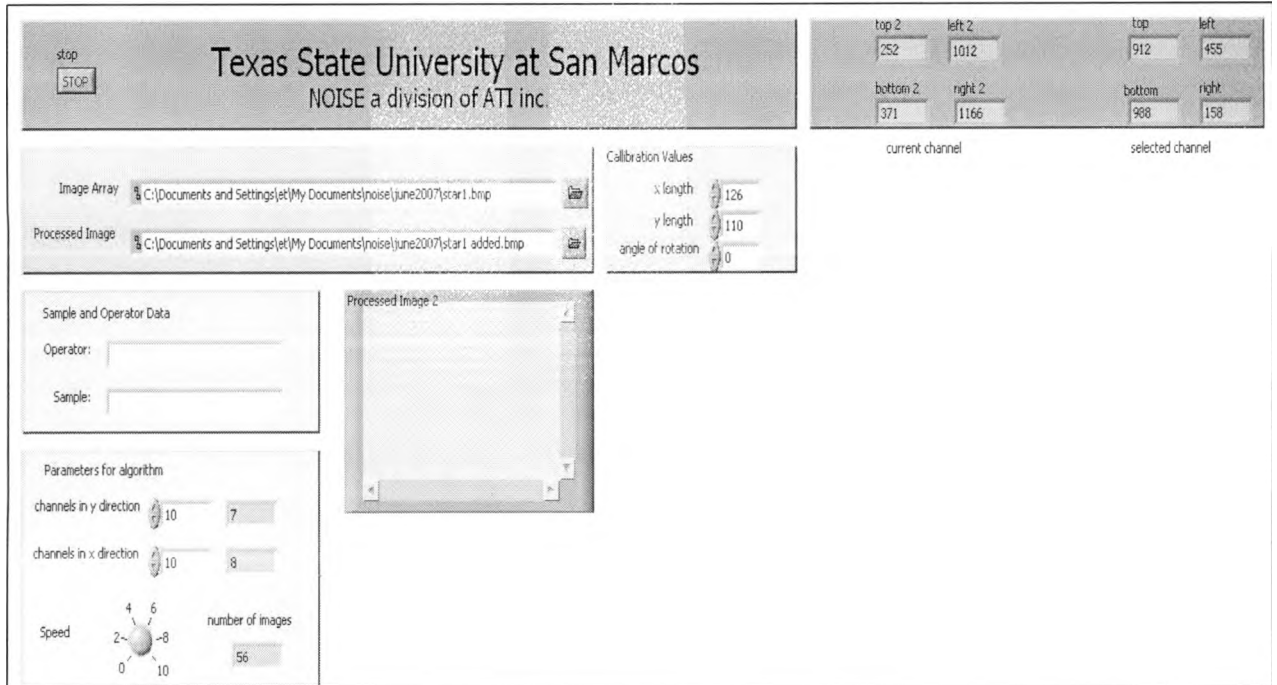


Figure 6.10: user interface for the 'shift and add' program, NOISE1.

The angle of rotation refers to whether the array is level or it is tilted. This comes from the physical orientation of the MLA. The rotation can be dealt with in several different ways. The best solution is to mount the MLA in a variable holder that rotates. This not

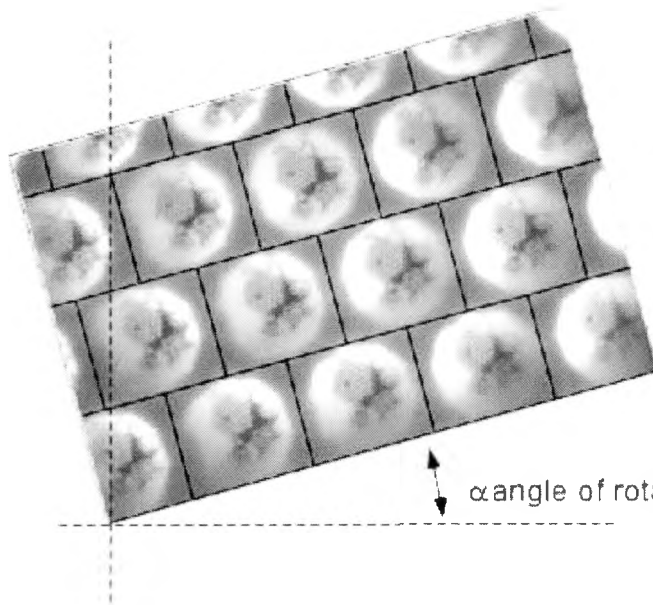


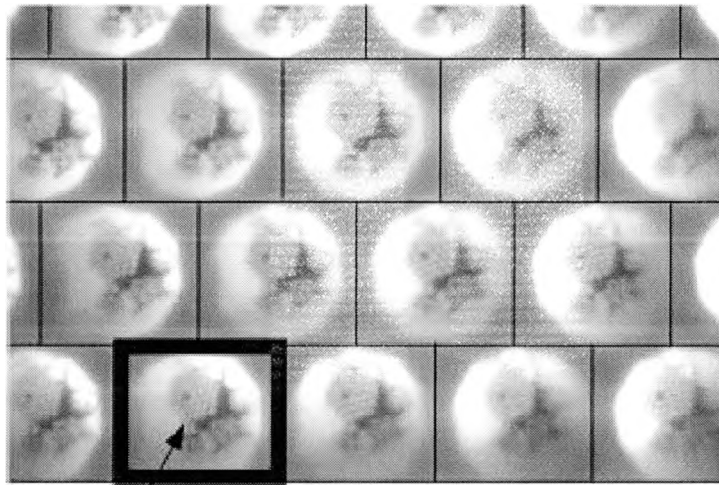
Figure 6.11: angle of rotation.

only makes the system easier to focus but allows the user to level the MLA, leaving the rotational factor unnecessary. If this is not an option, the angle of rotation in degrees with respect to the horizontal axis needs to be placed in the

'angle of rotation' input.

The 'grid calibration' and the 'shift and add' programs were kept separate because this more convenient when taking large amounts of data. There is also an input for how many channels are to be added in the x and y direction. This program will automatically tailor these numbers if they exceed the number of channels in the array. It will not know if there are channels in the array that should not be added, channels that are too dark or the edge effects of the MLA are too extreme. These problems can be bypassed by the physical setup of the system. The final setup that was used produces an array where every channel is usable. This does reduce the total number of channels. There is a compromise on whether the user wants to have more channels with the outer channels having questionable value or having fewer channels where the user does not have to worry about this. If the first option is chosen the user needs to be aware that using all the channels could decrease the contrast of the extracted image. Depending on the setup of the system, the user should use their own judgment for this input.

The first step in this program is the array is displayed and the user is prompted to select one rectangle in the lower left corner. This channel will be the lowest on the left edge that will be added.



Selected initial channel

Figure 6.12: the initial channel that the user selects needs to be in the bottom left corner.

This selection does not have to encompass the entire channel; it should include anything in the channel that the user is interested in. If there is any doubt about how much of the channel to select, there is no problem in selecting a larger area, the program will still shift the correct length. Once the initial channel is selected the program will add the indicated number of images and display then final summation. The user can slow this process to observe each image being added by adjusting the 'speed' knob. This can be a useful tool if the user is worried about the edge effects on some of the channels. The final image is saved under the pathway indicated under 'processed image'.

NOISE2.1 uses the same addition algorithm as NOISE1. It does not use the grid as a template like NOISE1 does. Instead it uses image registration techniques to obtain the coordinates of each channel.

CHAPTER 7

NOISE IN THE NEAR INFRARED

The images that were taken showed many different things. One is the difference between using a red or near infrared laser. Another is how the thicknesses of the front and back scatterers affect the final image. Images were also taken to find the optimal setting for N-IR NOISE.

7.1 Final Configuration

Several things were taken into consideration when deciding on the setup for the final data. It is desirable to keep as many images as possible, with the least amount of spread due to the MLA. These two things are limited by the MLA and lenses' position. Also, as much stray light as possible needed to be removed. An opening was left in the system for adjusting the scattering sample (chicken), so there was not way to avoid all stray light. The setup minimized this as best as possible by enclosing all the components that could be enclosed and turning off most of the background light when taking data.

Another problem was that light from each separate MLA impinged on each other, reducing the contrast of each image. This problem was solved using variable diaphragms. One diaphragm was placed in front of the MLA to keep the images from

overlapping. Another diaphragm was placed after the MLA to select only the center lenses for imaging.

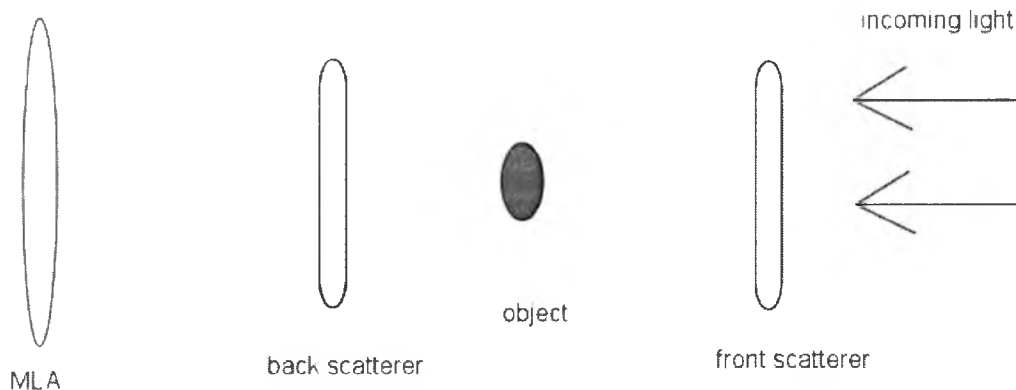


Figure 7.1: the front scatterer is the scattering element that is closest to the laser. The back scatterer is the scattering element closest to the camera.



The 808 nm laser was used to take pictures of a piece of copper embedded in chicken. The copper was shaped like a circle with a “hook”

Figure 7.2: coming out of one side. The “hook” on the side of the circle was the copper object with “hook”. feature that needed to be recognizable.

7.2 Voltage Variance

Pictures were taken with 1 cm of front scattering and half a cm of back scattering and varied the voltage, from 100mV to 800mV in 100mV steps. 100mV did not provide enough illumination for a clear picture but as little as 200mV provided a recognizable, if fuzzy, image.

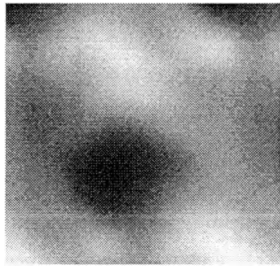


Figure 7.3: picture of hook taken with 100mV.

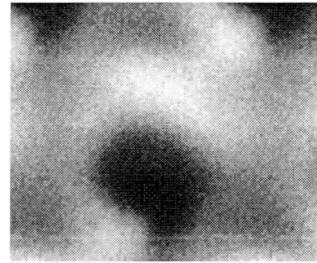


Figure 7.4: picture of hook taken with 200mV.

The image was clearest when 400 mV was used. As the voltage increased from here the image did not become much clearer. Everything greater than 400 mV did not improve the image significantly.

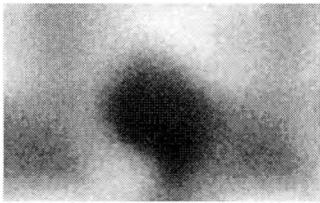


Figure 7.5: 400 mV.

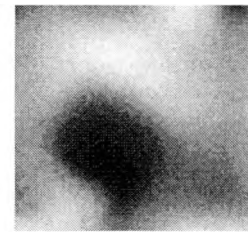


Figure 7.6: 800mV.

For safety reasons the lowest voltage setting (400 mV) was used that would still give a recognizable image for the rest of my measurements.

7.3 Thickness of the Scattering Medium

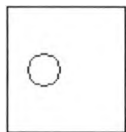


Figure 7.7: square object with a small identifying feature.

Then the effects of thickness of the scatterer were examined with respect to the thickness of back and front scattering. For this a square of copper with a hole punched in the center was used. I placed layers of chicken before and after the object without anything between the layers. Due to the nature of the chicken it was not possible to cut exact

thicknesses, each layer is approximately 3-5 mm.

At least 1 cm of front scattering is needed to maximize clarity, with anything more than that just decreasing the intensity of the light. This is because of the diffusing effect of the front scatterer, discussed in an earlier chapter.

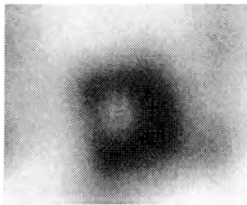


Figure 7.8: 4 layers of front scattering; 1 layer of back scattering.

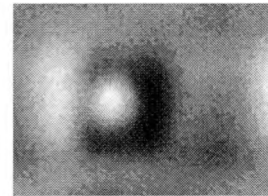


Figure 7.9: 2 layers of front scattering; 1 layer of back scattering.

The clarity decreases sharply when back scattering is increased.

Here just 1 layer of back scattering was added, bringing the total to 2 layers, and the hole in the square is completely obscured. This agrees with the theoretical model talked about in an earlier chapter.



Figure 7.10: 2 layers of chicken before and after then object, about 2.5 cm of chicken.

7.4 Red vs. Near Infrared

All these pictures were taken with an 808 nm laser. At this wavelength the chicken is more transparent than in the visible range. Several pictures were taken with a 685 nm diode laser to confirm this. The same type of chicken was used and a transparent sheet with an image printed on it was used for an object.

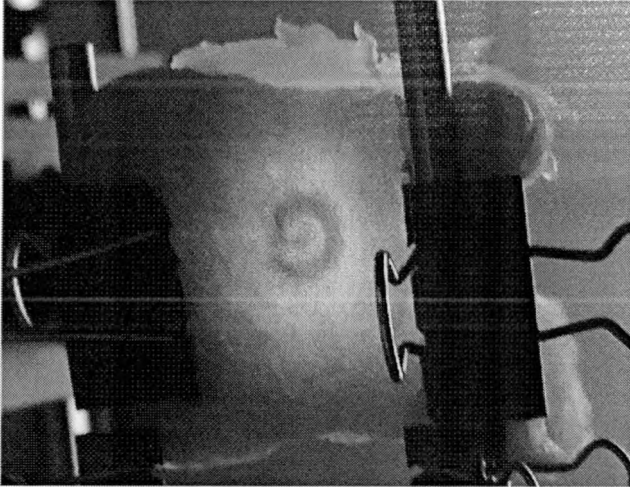


Figure 7.11: picture of object embedded in chicken illuminated by red laser.

The 'yoyo' can be clearly seen with a single piece of paper behind it.

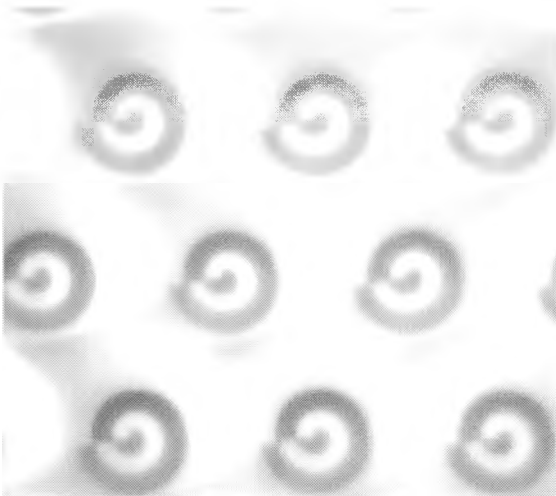


Figure 7.12: yoyo object with paper front scattering.

As with the N-IR laser at least 1 cm of chicken in front of the object is needed to make the object visible.

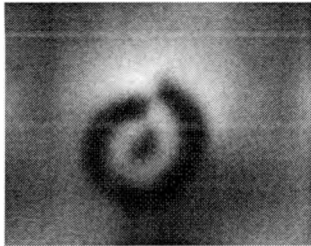


Figure 7.13: 2 layers of front scattering and 1 layer of back scattering

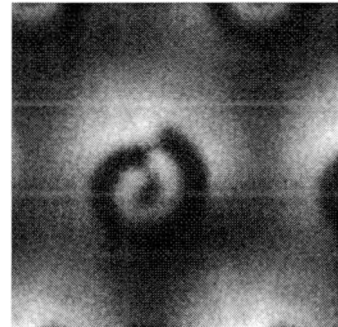


Figure 7.14: 4 layers of front scattering, 1 layer of back scattering

As the front scattering increases so does the clarity of the image as seen in Fig 8, and as back scattering increases the clarity decreases.

The intensity of the image decreases more quickly with the red laser than with the N-IR laser.



Figure 7.15: 3 layers of front scattering and 2 layers of back scattering taken with 685 nm laser

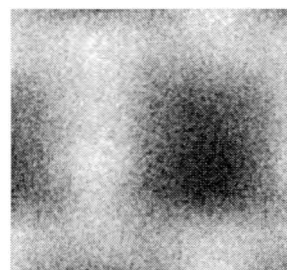


Figure 7.16: square object with 3 layers of front scattering and 2 layers of back scattering taken with 808 nm laser.

This relates to the absorption properties of biological tissue relating to the wavelength of the light. The light from the near infrared laser is not absorbed into the chicken as much as the light from the red laser.

CHAPTER 8

DISCUSSION AND CONCLUSIONS

This thesis describes the process of constructing a novel new system to image binary objects that are hidden in a scattering medium. The used imaging technique is Noninvasive Optical Imaging by Speckle Ensemble (NOISE). This technique was invented by Dr. Rosen from the Ben Gurion University of the Negev. The setup described in a setup very similar to the setup of Dr. Rosen but uses an infrared laser instead of a red laser and has different spatial constraints. This thesis addresses the concepts and peculiarities intrinsic in any NOISE system. Included is a thorough optical characterization of chicken breast used to map the therapeutic window.

We were successful in minimizing the floor plan of the NOISE setup, our construction being roughly one eighth of the size of Dr. Rosen's setup. We also successfully dealt with problems inherent in the field of view of the MLA caused by the shortened setup. We also explored optional setups that would maximize the number of channels available from the MLA. Variable apertures were suggested and tested as good solutions to some of the problems raised by the MLA. Further improvements to the setup include the installation of the beam splitter, integrating a visible laser into the setup making laser alignment easier.

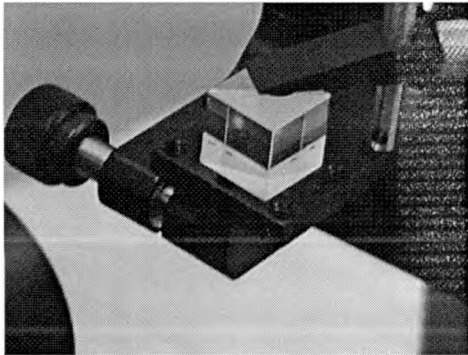


Figure 8.1: red laser directed at cubic beam splitter.

Two programs were written in LabView to extract images from the data. NOISE1 is user-friendly and extremely accurate. With the final setup it is extremely precise. It works with the live adding program to produce real-time images. Image registration software was also written to deal with MLA effects. Further improvements could be made to the real-time program to make it faster and more efficient.

Extensive characterization was performed on chicken breast as a representative of biological tissue. FTIR and filmetrics analysis was performed. Our results closely agree with previous research. As this project continues it may be necessary to characterize other types of biological tissue. A future avenue of research may contain using live tissue. Also, it might be beneficial to consider a way to exploit the agitation phenomenon mentioned in chapter six.

Images were taken with both red and near infrared lasers, comparing the difference in scattering properties of chicken with respect to wavelength. These images were taken with up to three cm of chicken meat. This is a thicker sample than the Rosen group used.

APPENDIX A

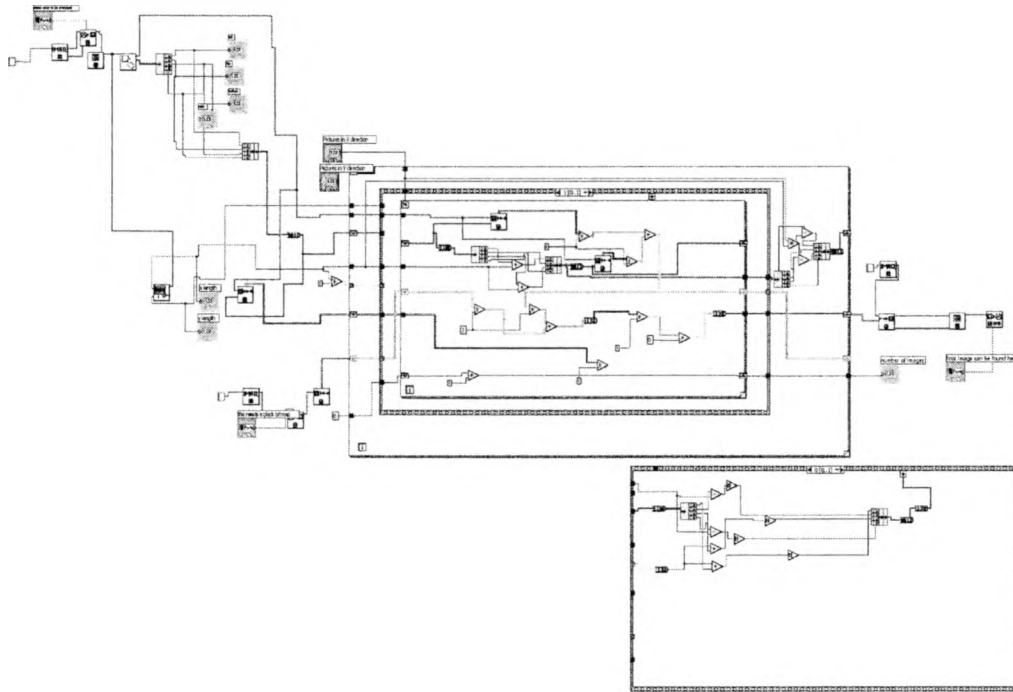
SYMBOLS

E	electric field
δ	phase
h	Planck's constant; $6.626068 \times 10^{-34} \text{ m}^2 \text{ kg / s}$
ν	frequency
T	temperature
k	Boltzmann's constant; $1.3806503 \times 10^{-23} \text{ m}^2 \text{ kg s}^{-2} \text{ K}^{-1}$
μ_a	absorption coefficient (cm^{-1})
ρ_a	volume density
σ_a	effective absorption cross-section (cm^2)
A	surface area
Q_a	absorption efficiency constant
μ_s	scattering coefficient (cm^{-1})
ρ_s	density of scatter center
σ_s	effective scattering cross-section (cm^2)
T_a	probability of absorption
L	length
T_s	probability of scattering
μ_s'	reduced scattering coefficient
g	anisotropy factor
ψ	azimuthal angle
n_p	refractive index
λ	wavelength
f	focal length
m	magnification
i	image distance
o	object distance

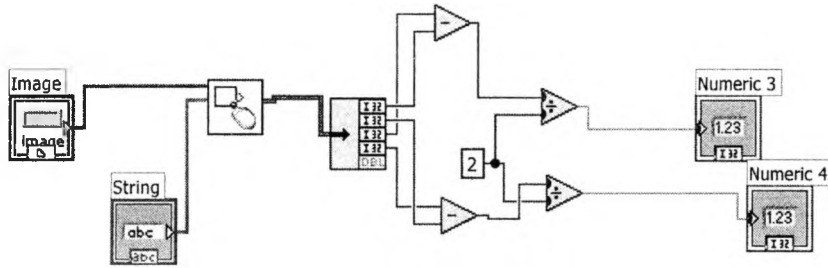
APPENDIX B

LABVIEW

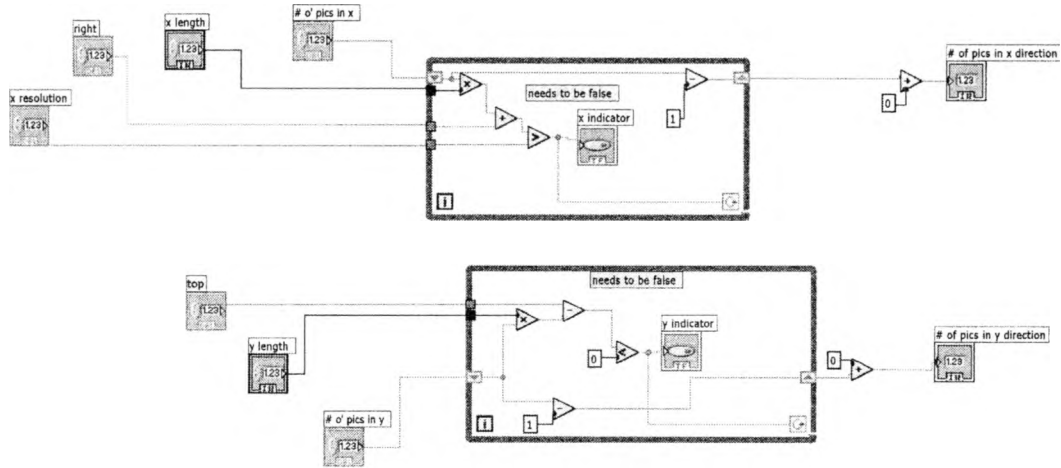
grid calibration and adding2.vi
C:\Documents and Settings\et\My Documents\noise\labview\grid calibration and adding2.vi
Last modified on 8/21/2006 at 5:57 PM
Printed on 7/18/2007 at 10:23 PM



grid lengths2.vi
C:\Documents and Settings\et\My Documents\noise\labview\grid lengths2.vi
Last modified on 6/23/2006 at 3:04 PM
Printed on 7/18/2007 at 10:23 PM



bound indicator1.vi
C:\Documents and Settings\et\My Documents\noise\labview\bound indicator1.vi
Last modified on 1/22/2007 at 5:49 PM
Printed on 7/18/2007 at 10:22 PM



WORKS CITED

- [1] J. Mourant, J. Freyer, A. Hielscher, A. Eick, D. Shen, "Mechanisms of light scattering from biological cells relevant to noninvasive optical-tissue diagnostics", *Applied Optics* vol. 37 No 16.
- [2] A. Dunn, C. Smithpeter, A. Welch, R. Richards-Kortum, "Finite-Difference Time-Domain Simulation of Light Scattering from Single Cells", *Journal of Biomedical Optics* vol 2 No 3.
- [3] R. Drezek, A. Dunn, R. Richards-Kortum, "Light scattering from cells: finite difference time-domain simulations and goniometric measurements", *Applied Optics* vol 38 No 16.
- [4] <http://en.wikipedia.org/wiki/MRI>.
- [5] http://en.wikipedia.org/wiki/Computed_tomography.
- [6] V. Tuchin, "Tissue Optics: Light Scattering Methods and Instruments for Medical Diagnosis," SPIE 2000.
- [7] http://en.wikipedia.org/wiki/Cell_nucleus.
- [8] <http://waynesword.palomar.edu/lmexer1a.htm#animal>.
- [9] PW Atkins, "Physical Chemistry", 1978, W.H. Freeman and Co.
- [10] <http://omlc.ogi.edu/classroom/ece532/class3/>.
- [11] R. Resnick., R. Eisberg, "Quantum Physics of Atoms, Molecules, Solids, Nuclei, and Particles, 2nd edition", 1985, John Wiley & Sons, New York.
- [12] A. K. Jain, "Fundamentals of digital image processing", 1989, Prentice-Hall Inc., New Jersey.
- [13] Gianandrea Mannarini, "Speckle Analysis of the Excitonic Emission from Quantum Wells", April 2005, Dissertation, University of Berlin.

- [14] J. Rosen, D. Abookasis, "Noninvasive optical imaging by speckle ensemble", Optics Letters vol 29 No 3.
- [15] V. Venugopalan, Beckman Laser Institute.

VITA

Elaine Elizabeth Tennant was born in Austin, Texas, on February 21, 1983, the daughter of Richard and Aimee Tennant. She was home schooled until the age of 15 when she attended Stephen F. Austin High School and graduated in May 2000. She went on to the University of Texas at Dallas where she earned a Bachelor of Science in Physics with a minor in Mathematics. After that she was accepted to Graduate Physics Department at the Texas State University-San Marcos. While earning her Masters of Science in Physics with a de facto minor in Mathematics she taught various physics labs. At both UTD and Texas State she participated in many outreach events including the Women in Physics Science Camp for Junior High Girls and the Physics Club at Hernandez Middle School in San Marcos.

Permanent Address: 3201 Nancy Gale

Austin, Texas 78735

This thesis was typed by Elaine Elizabeth Tennant.

